Supplementary Information for
A Highly Reactive $Co^{III,IV}_2(\mu\text{-}O)_2$ Diamond Core Complex that Cleaves C-H Bonds

Yan Li[1], Suhashini Handunneththige[2], Erik R. Farquhar[3,4], Yisong Guo[5], Marat R. Talipov[2]*, Feifei Li[2]* and Dong Wang[1]*

Materials and Methods

General Materials and Procedures. All chemicals are of the highest commercially available purity and used as received, unless noted otherwise. DHA-d_4 and fluorene-d_2 were prepared according to the procedures reported previously.[1] Hydrogen peroxide (H_2O_2, 30 wt % in H_2O), tetrabutylammonium hydroxide (TBAOH, 1.0 M in methanol), ceric ammonium nitrate (CAN), 9,10-dihydroanthracene (DHA), fluorene, cyclohexene, tetralin, ethylbenzene, ethylbenzene-d_{10}, naphthalene, ferrocene, acetylferrocene, diacetyl ferrocene, methanol and dichloromethane were purchased from Aldrich. DHA was re-crystalized twice from ethanol before use.

Physical Methods. ^{1}H NMR spectra were obtained with a Varian VNMRS 500 MHz spectrometer at -55 ^{o}C. UV-vis spectra were recorded on an Agilent Technologies Cary 8454 spectrometer equipped with a Unisoku USP-203-A cryostat for temperature control. GC-MS analysis was carried out on an Agilent Technologies 6890N GC system with a 5973 Mass selective detector. High-resolution ESI-MS spectra were obtained using an Agilent 6520 Accurate-Mass Q-TOF LC/MS. X-band (9.64 GHz) and S-band (3.50 GHz) EPR spectra were recorded on a Bruker Elexsys E-5100 spectrometer equipped with Oxford liquid helium cryostats. The quantification of all signals is relative to a Cu(II)-EDTA spin standard. The concentration of the standard was determined from an atomic absorption standard (Aldrich). For all instruments, the microwave frequency was calibrated with a frequency counter and the magnetic field with an NMR gaussmeter. A modulation frequency of 100 kHz was used for all EPR spectra. The spectral simulations were performed by using the SpinCount software.[2]

X-ray Absorption Spectroscopy.

Sample Preparation. All samples were prepared in methanol under the appropriate temperatures with the formation of the corresponding cobalt species confirmed by UV-vis spectroscopy. The samples were then transferred to and frozen in tandem Mössbauer/XAS holders having a 4 mm x 10 mm (VxH) window that was covered with 25.4μm thick Kapton tape. The corresponding EPR samples from the same batch of preparations were also made. The dicobalt species in these samples were pre-measured by EPR spectroscopy to determine the formation yields (typically >95% for **2** and ~70-80% for **3**) prior to XAS data collection. Yield corrected XANES spectrum of **3** was obtained by taking a scaled difference spectrum of **2** from **3**, i.e., [**3** - (**2***0.3)]/0.7.

Data Collection. X-ray absorption spectroscopy (XAS) experiments were carried out on beamline 7-3 of the Stanford Synchrotron Radiation Lightsource (SLAC National Accelerator Laboratory, Menlo Park, CA). The SPEAR3 storage ring operated at 3.0 GeV and 500mA in top-off mode. On beamline 7-3, a cryogenically cooled Si(220) (φ = 0°) double crystal monochromator was used for energy selection, and was detuned by 50% 1000 eV above the Co K-edge for harmonic rejection. A 32-element solid state germanium detector (Mirion Technologies) windowed on the Co Kα emission line was employed to measure fluorescence XAS spectra. Ge detector counts were maintained at <40 kHz / element, within the linear regime

of the detector amplifier electronics, with a Soller slit assembly and 3μ Fe_2O_3 filters placed between the sample and detector used to reduce count rates due to scatter. Data were typically acquired in 10 eV steps in the pre-edge region (1 sec. acquisition time), 0.3 eV steps along the edge (2 sec. acquisition time), and 0.05*k* steps in the EXAFS up to 15*k* (acquisition time increasing from 2-9 sec in a k^2 weighted fashion). A Co metal foil was measured concurrently for energy calibration, with the first inflection point of the foil spectrum set to 7709.0 eV. Sample temperatures were maintained at 10-15K using a closed cycle helium cryostat (Oxford Technologies). With the exception of **1**, all samples exhibited evidence of photoreduction during data collection. This manifested as a progressive red-shift of the absorption edge accompanied by changes in the shape and intensity of pre-edge and edge features. Consequently, single scans were collected on multiple non-overlapping spots on the sample. Only those scans showing consistency with one another and no evidence of photoreduction were used for data analysis.

Data Analysis. XAS data was inspected, calibrated and averaged using Athena.[3] X-ray Absorption Near Edge Spectroscopy (XANES) pre-edge peak fitting analysis was performed with Fityk,[4] using a modification of a previously reported methodology.[5] Briefly, 15-20 eV segments of the normalized XAS spectrum centered around the pre-edge peak were fit to a combination of a pseudo-Voigt function for the rising absorption edge and one or more pseudo-Voigt functions for the pre-edge peak. All pseudo-Voigt functions were constrained to a fixed 50:50 ratio of Gaussian:Lorentzian character. Extended X-ray Absorption Fine Structure (EXAFS) analysis was carried out using Artemis.[3] Structural models obtained by DFT calculations were used as FEFF6L input to determine theoretical phase and amplitude parameters as well as significant single-scattering paths to include in the fit model. For a given single-scattering shell in the model, the coordination number *n* was fixed, while *r* and σ^2 were allowed to float. The amplitude reduction factor S_0^2 was fixed at 0.9, while the edge shift parameter ΔE_0 was allowed to float at a single common value for all shells. The fit was evaluated in k^3-weighted R-space, and fit quality was judged by the reported R-factor and reduced χ^2.

Synthesis of ligand and the starting complex 1. The TPA ligand was synthesized following an established procedure.[6] Complex **1** was prepared according to the procedure reported previously, and was recrystallized twice from diethyl ether before use.[7]

Substrate oxidation by complex 3. Unless otherwise stated, all kinetic measurements were performed in a mixed solvent of 2:1 methanol/dichloromethane at -60 ^oC. CH_2Cl_2 was used to increase the solubility of substrates such as DHA and fluorene in methanol. In a typical experiment, an access amount of substrate (pre-dissolved in methanol/CH_2Cl_2 to make a stock solution) was added to a UV cuvette containing freshly prepared methanol solution of **3** using a micro-syringe. Under fast stirring, the change of the optical spectrum was monitored and recorded as a function of time. The time trace of the 480 nm band for each reaction was fitted using pseudo-first-order model to obtain the rate constant k_{obs}. For each substrate, a concentration-dependence experiment was carried out to measure k_{obs} under each substrate concentration. The plot of k_{obs} vs. substrate concentration was then fitted linearly to obtain the second order rate constant k_2.

$H_2{}^{18}O$ exchange kinetics. These experiments were performed in methanol at -60 ^oC on 3 mM diamond core complexes **2** or **3**.

To study $H_2{}^{18}O$ exchange at the stage of complex **2**, $H_2{}^{18}O$ of the target amount pre-mixed in a small amount of methanol was added into a freshly prepared solution of **2**. The resulting

solution was stirred for a period of incubation time (varied, up to 4 hours), and 3 equivalents of CAN was added to convert **2** to **3**, immediately followed by the addition of 0.5 mM ethylbenzene into the solution to react with **3**. After ethylbenzene oxidation was completed, the cobalt species was removed using a silica gel micro-column. Small amount of dichloromethane was used to wash the column and elute the organic product residual. The clear eluate was then concentrated and analyzed by GC-MS.

To study $H_2{}^{18}O$ exchange at the stage of complex **3**, $H_2{}^{18}O$ of the target amount pre-mixed in a small amount of methanol was added into a freshly prepared solution of **3**, immediately followed by the addition of 0.5 mM ethylbenzene into the solution to react with **3**. No incubation time was allowed due to the thermal instability of **3** ($t_{1/2}$ ~90 s at -60 ^{o}C).

Data analysis was performed using the Agilent MSD ChemStation software (version D.01.02.16). The GC peak corresponding to acetophenone was deconvoluted to reveal the ^{16}O and ^{18}O components using the "Extract Ion Chromatograms" function based on the MS fragments of 120 (^{16}O acetophenone), 105 (^{16}O acetophenone - CH_3), 122 (^{18}O acetophenone) and 107 (^{18}O acetophenone - CH_3). The ^{18}O incorporation percentage was calculated using the following equation:

$$^{18}O\% = \frac{^{18}O}{^{18}O + {}^{16}O} = \frac{A_{122}}{A_{122}+A_{120}} = \frac{A_{107}}{A_{107}+A_{105}}$$

where A_{122}, A_{120}, A_{107} and A_{105} represent the integration of the deconvoluted GC signal that corresponds to each MS fragment. The average value of $\frac{A_{122}}{A_{122}+A_{120}}$ and $\frac{A_{107}}{A_{107}+A_{105}}$ for each measurement was used to make plots shown in Figure 7 in the main text.

DFT calculations. Input models for **2** and **3** were built using Avogadro software and optimized using density functional theory (DFT) with the Gaussian 09, Revision E01 software.[8] Geometry optimization calculations were carried out with B3LYP, B3LYP*(15 % HF), M06-L and BP86 functionals in conjunction with 6-31G(D) basis set for all atoms.[9-15] Spin unrestricted geometry optimizations and frequency calculations were performed at 298.15 K with a polarized continuum solvent model (PCM) using methanol as the solvent. Wave function stability calculations were performed to ensure absence of lower-energy numerical solutions for the electronic structures of **2** and **3**.

References:

(1) Goldsmith, C. R.; Jonas, R. T.; Stack, T. D. P. C-H Bond Activation by a Ferric Methoxide Complex: Modeling the Rate-Determining Step in the Mechanism of Lipoxygenase. *J. Am. Chem. Soc.* **2002**, *124*, 83-96.

(2) Petasis, D. T.; Hendrich, M. P. Quantitative Interpretation of Multifrequency Multimode EPR Spectra of Metal Containing Proteins, Enzymes, and Biomimetic Complexes. *Methods Enzymol.* **2015**, *563*, 171-208.

(3) Ravel, B.; Newville, M. ATHENA, ARTEMIS, HEPHAESTUS: Data Analysis for X-ray Absorption Spectroscopy Using IFEFFIT. *J. Synchrotron Radiat.* **2005**, *12*, 537-541.

(4) Wojdyr, M. Fityk: A General-purpose Peak Fitting Program. *J. Appl. Cryst.* **2010**, *43*, 1126-1128.

(5) Westre, T. E.; Kennepohl, P.; DeWitt, J. G.; Hedman, B.; Hodgson, K. O.; Solomon, E. I. A Multiplet Analysis of Fe K-Edge 1s -> 3d Pre-Edge Features of Iron Complexes. *J. Am. Chem. Soc.* **1997**, *119*, 6297-6314.

(6) Zhang, C. X.; Kaderli, S.; Costas, M.; Kim, E.-i.; Neuhold, Y.-M.; Karlin, K. D.; Zuberbuhler, A. D. Copper(I)-Dioxygen Reactivity of $[(L)CuI]^+$ (L = Tris(2-pyridylmethyl)amine): Kinetic/Thermodynamic and Spectroscopic Studies Concerning the Formation of Cu-O_2 and Cu_2-O_2 Adducts as a Function of

Solvent Medium and 4-Pyridyl Ligand Substituent Variations. *Inorg. Chem.* **2003**, *42*, 1807-1824.
(7) Chan, S. L.-F.; Lam, T. L.; Yang, C.; Lai, J.; Cao, B.; Zhou, Z.; Zhu, Q. Cobalt(II) Tris(2-pyridylmethyl)amine Complexes $[Co(TPA)X]^+$ Bearing Coordinating Anion (X = Cl , Br , I and NCS): Synthesis and Application for Carbon Dioxide Reduction. *Polyhedron* **2017**, *125*, 156-163.
(8) Gaussian 09, Revision A.01, Frisch, M. J.; Trucks, G. W.; Schlegel, H. B.; Scuseria, G. E.; Robb, M. A.; Cheeseman, J. R.; Scalmani, G.; Barone, V.; Mennucci, B.; Petersson, G. A.; Nakatsuji, H.; Caricato, M.; Li, X.; Hratchian, H. P.; Izmaylov, A. F.; Bloino, J.; Zheng, G.; Sonnenberg, J. L.; Hada, M.; Ehara, M.; Toyota, K.; Fukuda, R.; Hasegawa, J.; Ishida, M.; Nakajima, T.; Honda, Y.; Kitao, O.; Nakai, H.; Vreven, T.; Montgomery, J. A., Jr.; Peralta, J. E.; Ogliaro, F.; Bearpark, M.; Heyd, J. J.; Brothers, E.; Kudin, K. N.; Staroverov, V. N.; Kobayashi, R.; Normand, J.; Raghavachari, K.; Rendell, A.; Burant, J. C.; Iyengar, S. S.; Tomasi, J.; Cossi, M.; Rega, N.; Millam, J. M.; Klene, M.; Knox, J. E.; Cross, J. B.; Bakken, V.; Adamo, C.; Jaramillo, J.; Gomperts, R.; Stratmann, R. E.; Yazyev, O.; Austin, A. J.; Cammi, R.; Pomelli, C.; Ochterski, J. W.; Martin, R. L.; Morokuma, K.; Zakrzewski, V. G.; Voth, G. A.; Salvador, P.; Dannenberg, J. J.; Dapprich, S.; Daniels, A. D.; Farkas, Ö.; Foresman, J. B.; Ortiz, J. V.; Cioslowski, J.; Fox, D. J. Gaussian, Inc., Wallingford CT, **2009**.
(9) Perdew, J. P. Density-Functional Approximation for the Correlation Energy of the Inhomogeneous Electron Gas. *Phys. Rev. B* **1986**, *33*, 8822-8824.
(10) Becke, A. D. Density-Functional Exchange-Energy Approximation with Correct Asymptotic Behavior. *Phys. Rev. A* **1988**, *38*, 3098-3100.
(11) Becke, A. D. Density-functional Thermochemistry. III. The Role of Exact Exchange. *J. Chem. Phys.* **1993**, *98*, 5648-5652.
(12) Zhao, Y.; Truhlar, D. G. A New Local Density Functional for Main-group Thermochemistry, Transition Metal Bonding, Thermochemical Kinetics, and Noncovalent Interactions. *J. Chem. Phys.* **2006**, *125*, 1-18.
(13) Salomon, O.; Reiher, M.; Hess, B. A. Assertion and Validation of the Performance of the B3LYP⋆ Functional for the First Transition Metal Row and the G2 Test Set. *J. Chem. Phys.* **2002**, *117*, 4729-4737.
(14) Francl, M. M.; Pietero, W. J.; Hehre, W. J.; Binkley, J. S.; Gordon, M. S.; DeFrees, D. J.; Pople, J. A. Self-consistent Molecular Orbital Methods. XXIII. A Polarization-type Basis Set for Second-row Elements. *J. Chem. Phys.* **1982**, *77*, 3654.
(15) Rassolov, V. A.; Pople, J. A.; Ratner, M. A.; Windus, T. L. 6-31G* Basis Set for Atoms K Through Zn. *J. Chem. Phys.* **1998**, *109*, 1223.
(16) Zang, Y.; Dong, Y.; Que, L., Jr.; Kauffmann, K.; Münck, E. The First Bis(μ-oxo)diiron(III) Complex. Structure and Magnetic Properties of $[Fe_2(\mu\text{-}O)_2(6TLA)_2](C1O_4)_2$. *J. Am. Chem. Soc.* **1995**, *117*, 1169-1170.
(17) Zheng, H.; Zang, Y.; Dong, Y.; Young, V. G., Jr.; Que, L., Jr.,. Complexes with $Fe^{III}_2(\mu\text{-}O)$(μ-OH), $Fe^{III}_2(\mu\text{-}O)_2$, and $Fe^{III}_3(\mu\text{-}O)_3$ Cores: Structures, Spectroscopy, and Core Interconversions. *J. Am. Chem. Soc.* **1999**, *121*, 2226-2235.
(18) Hsu, H.-F.; Dong, Y.; Shu, L.; Young, V. G., Jr. ; Que, L., Jr. Crystal Structure of a Synthetic High-Valent Complex with an $Fe_2(\mu\text{-}O)_2$ Diamond Core. Implications for the Core Structures of Methane Monooxygenase Intermediate Q and Ribonucleotide Reductase Intermediate X. *J. Am. Chem. Soc.* **1999**, *121*, 5230-5237.
(19) Xue, G.; Wang, D.; De Hont, R.; Fiedler, A. T.; Shan, X.; Münck, E.; Que, L., Jr. A Synthetic Precedent for the $[Fe^{IV}_2(\mu\text{-}O)_2]$ Diamond Core Proposed for Methane Monooxygenase Intermediate **Q**. *Proc. Natl. Acad. Sci. USA* **2007**, *104*, 20713-20718.
(20) Hitomi, Y.; Ando, A.; Matsui, H.; Ito, T.; Tanaka, T.; Ogo, S.; Funabiki, T. Aerobic Catechol Oxidation Catalyzed by a Bis(μ-oxo)dimanganese(III,III) Complex via a Manganese(II)−Semiquinonate Complex. *Inorg. Chem.* **2005**, *44*, 3473-3478.
(21) Towle, D. K.; Botsford, C. A.; Hodgson, D. J. Synthesis and Characterization of the Binuclear Mixed Valence Complex Di-μ-oxobis[tris(2-methyl-pyridyl)amine] Dimanganese(III, IV) Dithionate Heptahydrate, $[(tpa)MnO]_2(S_2O_6)_{3/2}\cdot 7H_2O$. *Inorg. Chim. Acta* **1988**, *141*, 167-168.

(22) Stebler, M.; Ludi, A.; Buergi, H. B. $[(phen)_2Mn^{IV}(\mu\text{-}O)_2Mn^{III}(phen)_2](PF_6)_3 \bullet CH_3CN$ and $[(phen)_2Mn^{IV}(\mu\text{-}O)_2Mn^{IV}(phen)_2](ClO_4)_4 \bullet CH_3CN$ (phen = 1,10-Phenanthroline): Crystal Structure Analyses at 100 K, Interpretation of Disorder, and Optical, Magnetic, and Electrochemical Results. *Inorg. Chem.* **1986**, *25*, 4743-4750.
(23) Engelmann, X.; Yao, S.; Farquhar, E. R.; Szilvμsi, T.; Kuhlmann, U.; Hildebrandt, P.; Driess, M.; Ray, K. A New Domain of Reactivity for High-Valent Dinuclear $[M(\mu\text{-}O)_2M']$ Complexes in Oxidation Reactions. *Angew. Chem. Int. Ed.* **2017**, *56*, 297-301.
(24) Dai, X.; Kapoor, P.; Warren, T. H. $[Me_2NN]Co(\eta^6\text{-toluene})$: O=O, N=N, and O=N Bond Cleavage Provides β-Diketiminato Cobalt μ-Oxo and Imido Complexes. *J. Am. Chem. Soc.* **2004**, *126*, 4798-4799.
(25) Zhao, P.; Lei, H.; Ni, C.; Guo, J.-D.; Kamali, S.; Fettinger, J. C.; Grandjean, F.; Long, G. J.; Nagase, S.; Power, P. P. Quasi-Three-Coordinate Iron and Cobalt Terphenoxide Complexes $\{Ar^{iPr8}OM(\mu\text{-}O)\}_2$ (Ar^{iPr8} = C_6H-2,6-(C_6H_2-2,4,6-iPr$_3$)$_2$-3,5-iPr$_2$; M = Fe or Co) with $M(III)_2(\mu\text{-}O)_2$ Core Structures and the Peroxide Dimer of 2-Oxepinoxy Relevant to Benzene Oxidation. *Inorg. Chem.* **2015**, *54*, 8914-8922.
(26) Hikichi, S.; Yoshizawa, M.; Sasakura, Y.; Akita, M.; Moro-oka, Y. First Synthesis and Structural Characterization of Dinuclear M(III) Bis(μ-oxo) Complexes of Nickel and Cobalt with Hydrotris(pyrazolyl)borate Ligand. *J. Am. Chem. Soc.* **1998**, *120*, 10567-10568.
(27) Larsen, P. L.; Parolin, T. J.; Powell, D. R.; Hendrich, M. P.; Borovik, A. S. Hydrogen Bonds around $M(m\text{-}O)_2M$ Rhombs: Stabilizing a $\{Co^{III}(\mu\text{-}O)_2Co^{III}\}$ Complex at Room Temperature. *Angew. Chem. Int. Ed.* **2003**, *42*, 85-89.
(28) DeRosha, D. E.; Mercado, B. Q.; Lukat-Rodgers, G.; Rodgers, K. R.; Holland, P. L. Enhancement of C-H Oxidizing Ability in $Co–O_2$ Complexes through an Isolated Heterobimetallic Oxo Intermediate. *Angew. Chem. Int. Ed.* **2017**, *56*, 3211-3215.
(29) Shiren, K.; Ogo, S.; Fujinami, S.; Hayashi, H.; Suzuki, M.; Uehara, A.; Watanabe, Y.; Moro-oka, Y. Synthesis, Structures, and Properties of Bis(μ-oxo)nickel(III) and Bis(μ-superoxo)nickel(II) Complexes: An Unusual Conversion of a $Ni^{III}_2(\mu\text{-}O)_2$ Core into a $Ni^{II}_2(\mu\text{-}OO)_2$ Core by H_2O_2 and Oxygenation of Ligand. *J. Am. Chem. Soc.* **2000**, *122*, 254-262.
(30) Cho, J.; Furutachi, H.; Fujinami, S.; Tosha, T.; Ohtsu, H.; Ikeda, O.; Suzuki, A.; Nomura, M.; Uruga, T.; Tanida, H.; Kawai, T.; Tanaka, K.; Kitagawa, T.; Suzuki, M. Sequential Reaction Intermediates in Aliphatic C-H Bond Functionalization Initiated by a Bis(μ-oxo)dinickel(III) Complex. *Inorg. Chem.* **2006**, *45*, 2873-2885.
(31) Hayashi, H.; Fujinami, S.; Nagatomo, S.; Ogo, S.; Suzuki, M.; Uehara, A.; Watanabe, Y.; Kitagawa, T. A Bis(μ-oxo)dicopper(III) Complex with Aromatic Nitrogen Donors: Structural Characterization and Reversible Conversion between Copper(I) and Bis(μ-oxo)dicopper(III) Species. *J. Am. Chem. Soc.* **2000**, *122*, 2124-2125.
(32) Ishizuka, T.; Watanabe, A.; Kotani, H.; Hong, D.; Satonaka, K.; Wada, T.; Shiota, Y.; Yoshizawa, K.; Ohara, K.; Yamaguchi, K.; Kato, S.; Fukuzumi, S.; Kojima, T. Homogeneous Photocatalytic Water Oxidation with a Dinuclear Co^{III}−Pyridylmethylamine Complex. *Inorg. Chem.* **2016**, *55*, 1154-1164.
(33) Wang, H.-Y.; Mijangos, E.; Ott, S.; Thapper, A. Water Oxidation Catalyzed by a Dinuclear Cobalt–Polypyridine Complex. *Angew. Chem. Int. Ed.* **2014**, *53*, 14499-14502.
(34) Kotani, H.; Hong, D.; Satonaka, K.; Ishizuka, T.; Kojima, T. Mechanistic Insight into Dioxygen Evolution from Diastereomeric μ-Peroxo Dinuclear Co(III) Complexes Based on Stoichiometric Electron-Transfer Oxidation. *Inorg. Chem.* **2019**, *58*, 3676-3682.
(35) Park, G. Y.; Qayyum, M. F.; Woertink, J.; Hodgson, K. O.; Hedman, B.; Sarjeant, A. A. N.; Solomon, E. I.; Karlin, K. D. Geometric and Electronic Structure of $[\{Cu(MeAN)\}_2(\mu\text{-}\eta^2\text{:}\eta^2(O_2^{2-}))]^{2+}$ with an Unusually Long O−O Bond: O−O Bond Weakening vs Activation for Reductive Cleavage. *J. Am. Chem. Soc.* **2012**, *134*, 8513-8524.
(36) Xue, G.; Pokutsa, A.; Que, L., Jr. Substrate-Triggered Activation of a Synthetic $[Fe_2(\mu\text{-}O)_2]$ Diamond Core for C−H Bond Cleavage. *J. Am. Chem. Soc.* **2011**, *133*, 16657-16667.
(37) Larsen, A. S.; Wang, K.; Lockwood, M. A.; Rice, G. L.; Won, T.-J.; Lovell, S.; Sadılek, M.; Turecek, F.; Mayer, J. M. Hydrocarbon Oxidation by Bis-μ-oxo Manganese Dimers: Electron Transfer, Hydride

Transfer, and Hydrogen Atom Transfer Mechanisms. *J. Am. Chem. Soc.* **2002**, *124*, 10112-10123.
(38) Wang, K.; Mayer, J. M. Oxidation of Hydrocarbons by $[(phen)_2Mn(\mu\text{-}O)_2Mn(phen)_2]^{3+}$ via Hydrogen Atom Abstraction. *J. Am. Chem. Soc.* **1997**, *119*, 1470-1471.
(39) Matsumoto, T.; Ohkubo, K.; Honda, K.; Yazawa, A.; Furutachi, H.; Fujinami, S.; Fukuzumi, S.; Suzuki, M. Aliphatic C−H Bond Activation Initiated by a (μ-η^2:η^2-Peroxo)dicopper(II) Complex in Comparison with Cumylperoxyl Radical. *J. Am. Chem. Soc.* **2009**, *131*, 9258-9267.
(40) Xue, G.; Hont, R. D.; Münck, E.; Que, L., Jr. Million-fold Activation of the $[Fe_2(\mu\text{-}O)_2]$ Diamond Core for C−H Bond Cleavage. *Nat. Chem.* **2010**, *2*, 400-405.
(41) Hong, S.; Pfaff, F. F.; Kwon, E.; Wang, Y.; Seo, M.-S.; Bill, E.; Ray, K.; Nam, W. Spectroscopic Capture and Reactivity of a Low-Spin Cobalt(IV)-Oxo Complex Stabilized by Binding Redox-Inactive Metal Ions. *Angew. Chem. Int. Ed.* **2014**, *53*, 10403-10407.
(42) Wang, B.; Lee, Y.-M.; Tcho, W.-Y.; Tussupbayev, S.; Kim, S.-T.; Kim, Y.; Seo, M. S.; Cho, K.-B.; Dede, Y.; Keegan, B. C.; Ogura, T.; Kim, S. H.; Ohta, T.; Baik, M.-H.; Ray, K.; Shearer, J.; Nam, W. Synthesis and Reactivity of a Mononuclear Non-haem Cobalt(IV)-oxo Complex. *Nat. Commun.* **2017**, *8*, 14839.

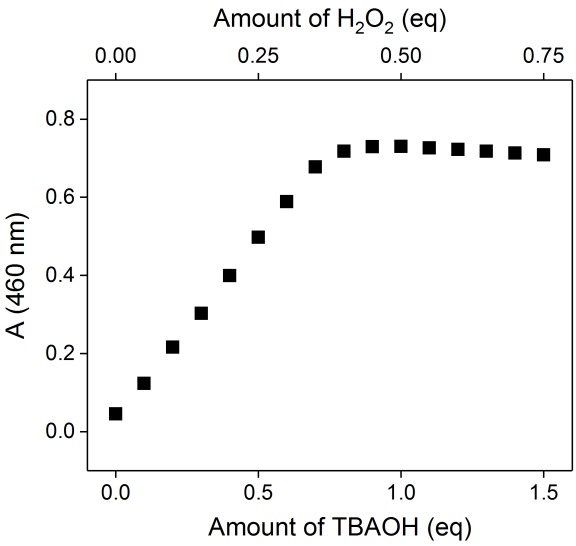

Figure S1. Titration of the formation of **2** monitored at 460 nm as a function of the amount of H_2O_2/OH^- added. The ratio of H_2O_2:OH^- was kept at 1:2 for the entire experiment.

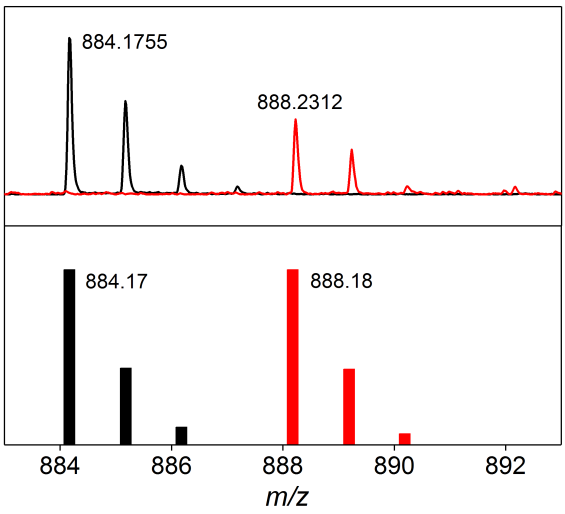

Figure S2. Experimental (top) and simulated (bottom) ESI-MS spectra of **2**-^{16}O (black) and **2**-^{18}O (red).

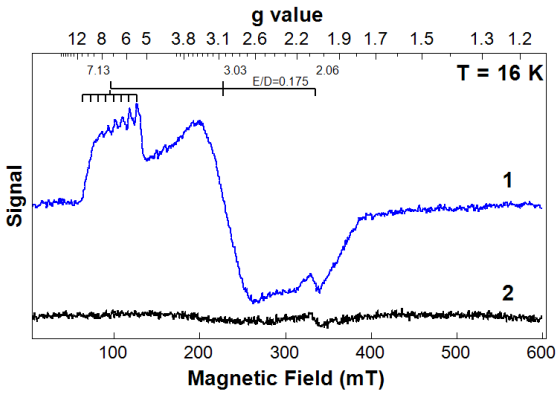

Figure S3. X-band EPR spectra of **1** and **2** recorded at 16 K. The EPR signal from complex **1** is originated from the $m_S = \pm 1/2$ Kramer's doublet of an $S = 3/2$ spin system with E/D = 0.175 determined by the observed effective g values. The hyperfine splitting pattern from ^{59}Co nucleus is clearly observed for $g_{eff} = 7.13$ resonance. For complex **2**, it is EPR silent.

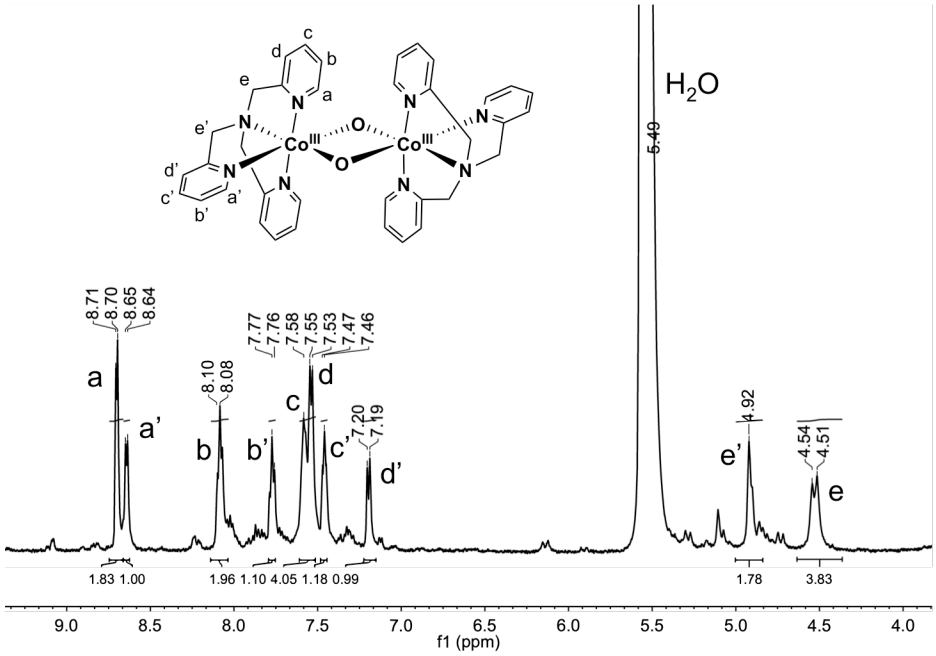

Figure S4. ^{1}H NMR of **2** obtained at -55 ^{o}C in methanol.

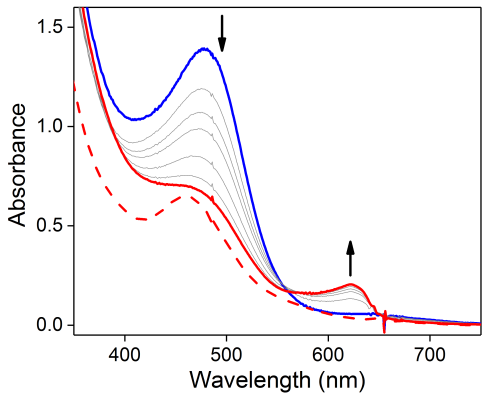

Figure S5. Reduction of **3** (blue) by ferrocene, showing the formation of **2** at 460 nm and the ferrocenium cation at 622 nm (solid red). The spectrum of the original **2** (dashed red) is also shown for comparison.

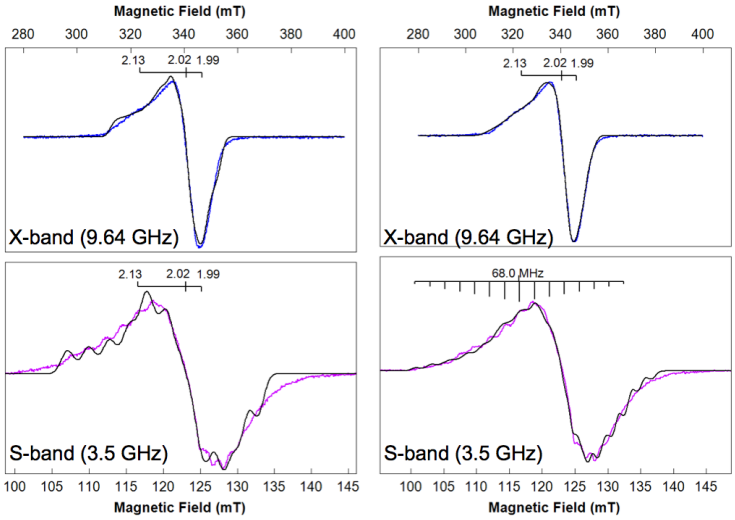

Figure S6. 16 K EPR spectra of complex **3** measured under X- (blue) and S-band (purple) frequencies and the simulations derived from different models. The hyperfine splitting pattern, which is clearly visible at the lower field region of the EPR resonance in the S-band data (along g_1 = 2.13 resonance), is consistent with a pattern involving two ^{59}Co nuclei with almost identical A value having a magnitude ~70 MHz as indicated in the bottom right spectrum. Left: The simulation used a single ^{59}Co nucleus with the simulation parameters: g = [2.13, 2.02, 1.99], σ_g = [0.01, 0.008, 0.008], A(^{59}Co) = [88, 40, 10] MHz, and Euler angle [α, β, γ] = [7°, 30°, 0], line width = 0.7 mT. The single ^{59}Co A tensor simulation cannot reproduce the hyperfine splitting pattern observed in the S-band data correctly. Right: The simulation used two independent ^{59}Co nuclei with the simulation parameters: g = [2.13, 2.02, 1.99], σ_g = [0.01, 0.008, 0.008], A_1(^{59}Co) = [78, 35, 20] MHz, and Euler angle [α, β, γ] = [0, 10°, 0], A_2(^{59}Co) = [64, 35, 5] MHz, and Euler angle [α, β, γ] = [0, 30°, 0], line width = 0.7 mT. The simulation reproduces the overall shape of the spectra in both S- and X-bands, but the simulated hyperfine splitting pattern does not reproduce the experimental data as well as the simulation shown in Figure 2, which assumes two identical ^{59}Co nuclei.

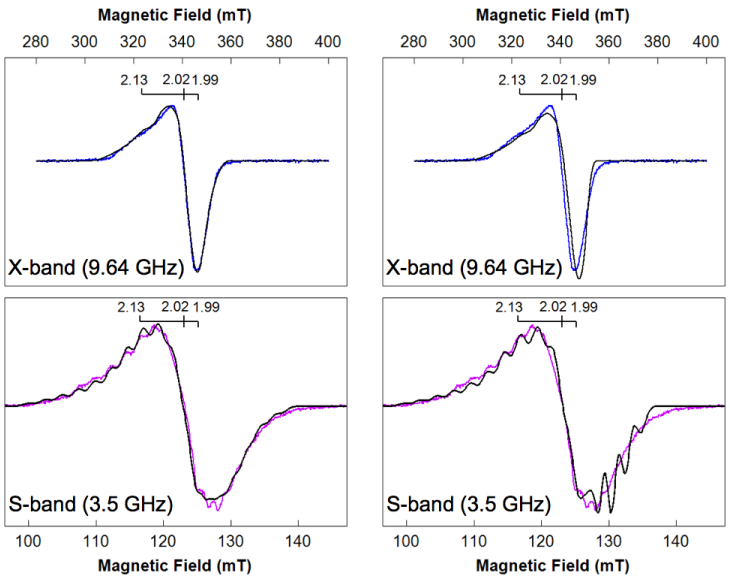

Figure S7. 16 K EPR spectra of complex **3** measured under X- (blue) and S-band (purple) frequencies and the simulations derived from different models. Left: a simulation assuming two identical ^{59}Co nuclei with an Euler angle of $\beta = 20^{o}$. Right: a simulation assuming two identical ^{59}Co nuclei without the inclusion of Euler angles.

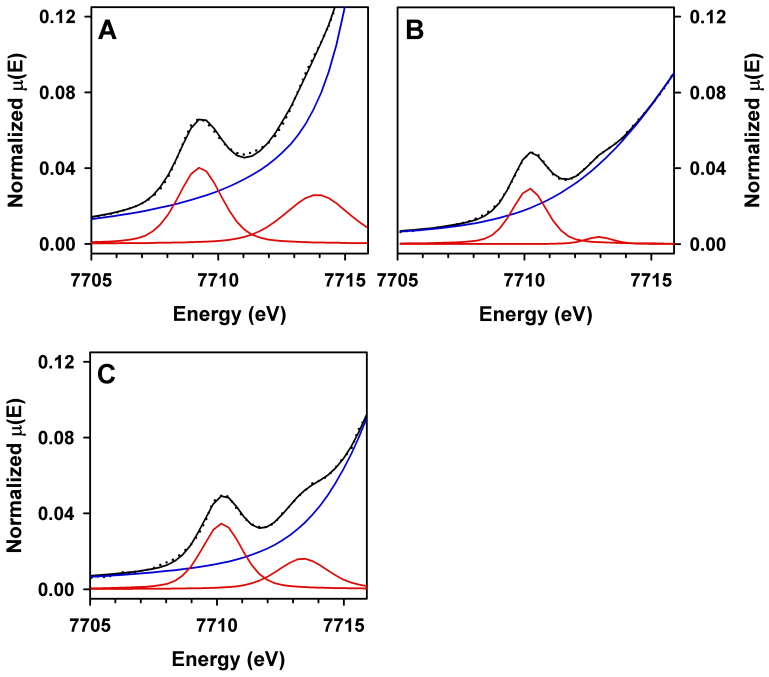

Figure S8. Representative pre-edge peak fits of **1** (panel A), **2** (panel B) and **3** (panel C). The spectrum in Panel C shows the raw data without correction for the formation yield of **3**.

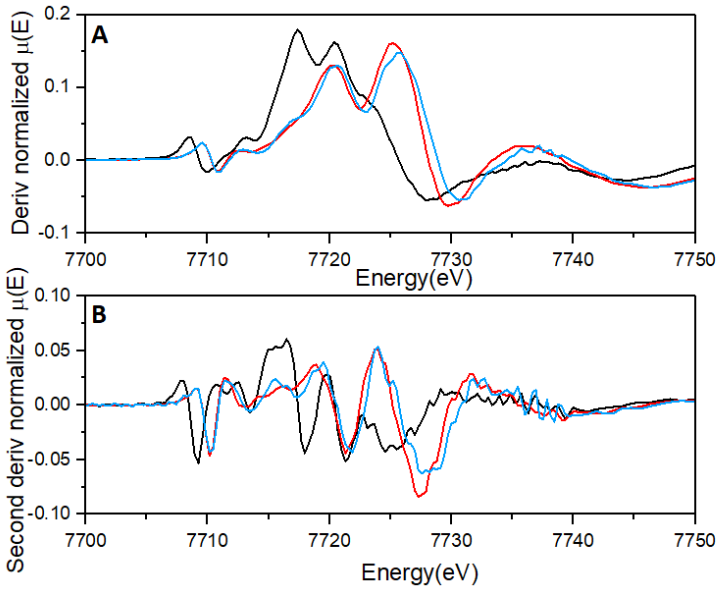

Figure S9. First derivative (panel A) and second derivative (panel B) of the normalized XANES spectra of **1** (black), **2** (red) and **3** (blue).

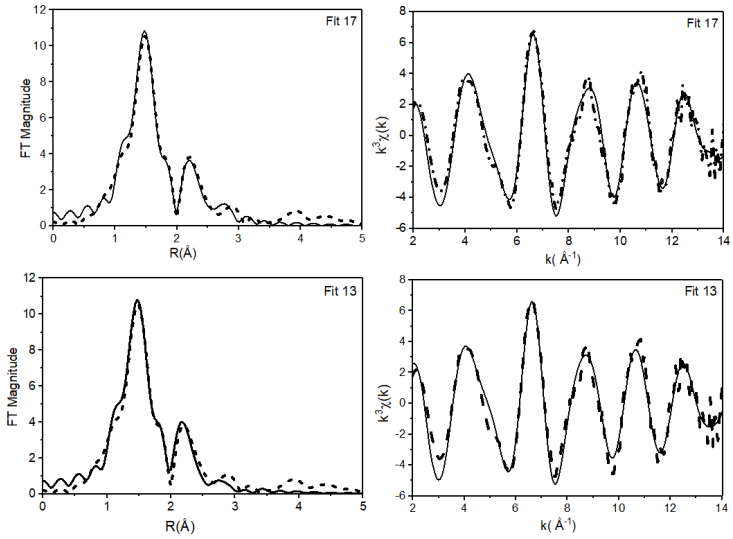

Figure S10. Comparison of Fourier transforms of the Co K-edge EXAFS data (left) and unfiltered EXAFS spectra (k^3 $\chi(k)$, right) for complex **2** with (fit 17) and without (fit 13) a cobalt scatterer. Experimental data are shown with dash (---) lines and fits with solid (——) lines. k = 2 – 14 Å^{-1}. Fit parameters for stated fits are shown in Table S1.

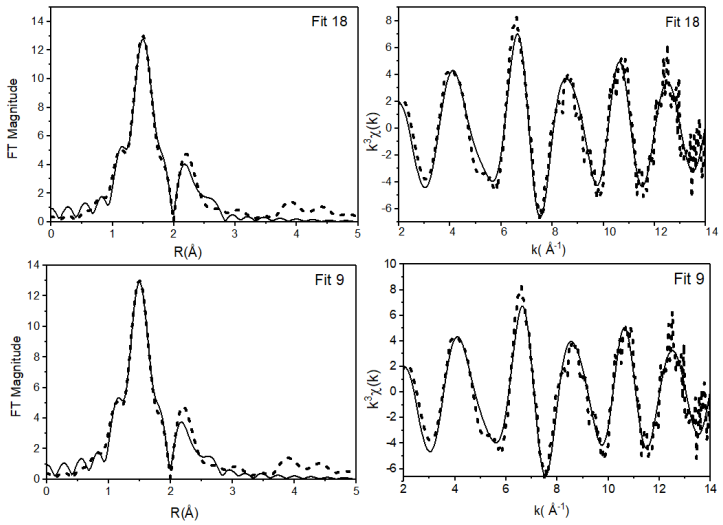

Figure S11. Comparison of Fourier transforms of the Co K-edge EXAFS data (left) and unfiltered EXAFS spectra (k^3 $\chi(k)$, right) for complex **3** with (fit 18) and without (fit 9) a cobalt scatterer. Experimental data are shown with dash (---) lines and fits with solid (——) lines. k = 2 – 14 Å^{-1}. Fit parameters for stated fits are shown in Table S2.

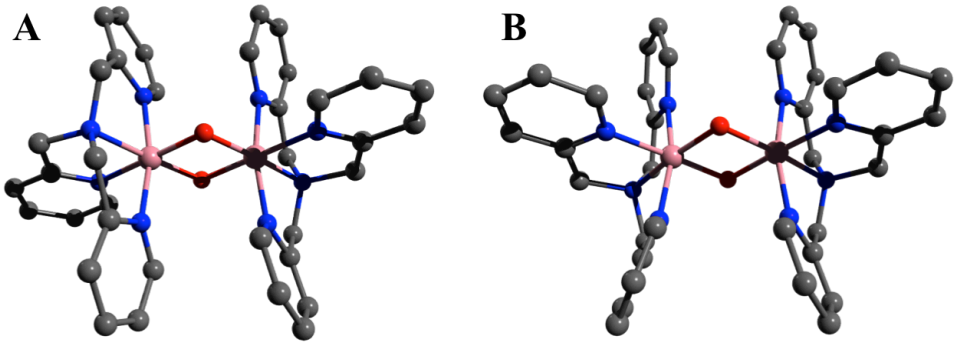

Figure S12: BP86/6-31G(D) optimized symmetric diamond core structures for **2** in the *trans*- (panel A) and *cis*- (panel B) configuration. Cobalt: pink, oxygen: red, nitrogen: blue, carbon: gray, hydrogen atoms are omitted for clarity.

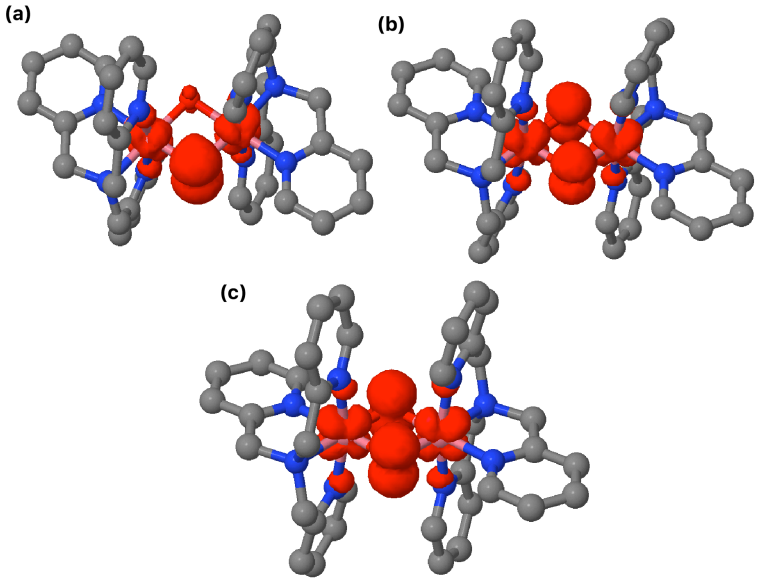

Figure S13: Spin density plots of **3** obtained with a) B3LYP/6-31G(D), b) B3LYP*(15% HF)/6-31G(D), c) M06-L/6-31G(D) using the polarized continuum model with the methanol parameters.

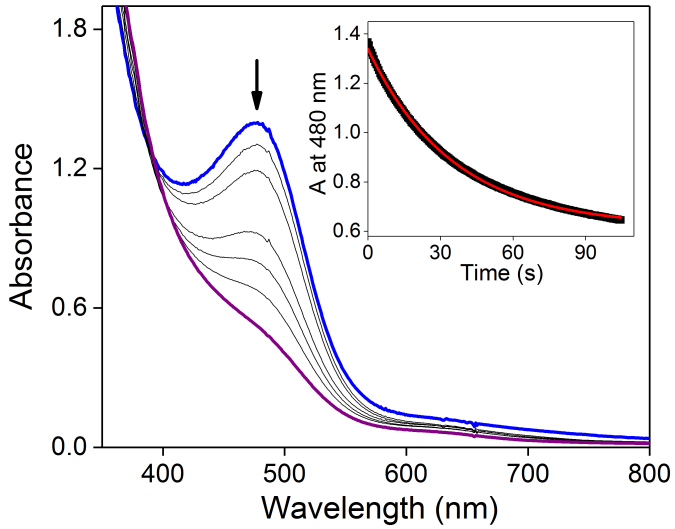

Figure S14. Change of the optical spectrum of 0.1 mM **3** (blue) in the course of reaction with 8 mM DHA at -60 ^{o}C. Inset: time trace of the absorption maximum at 480 nm, best fitted to a first-order exponential decay (red curve).

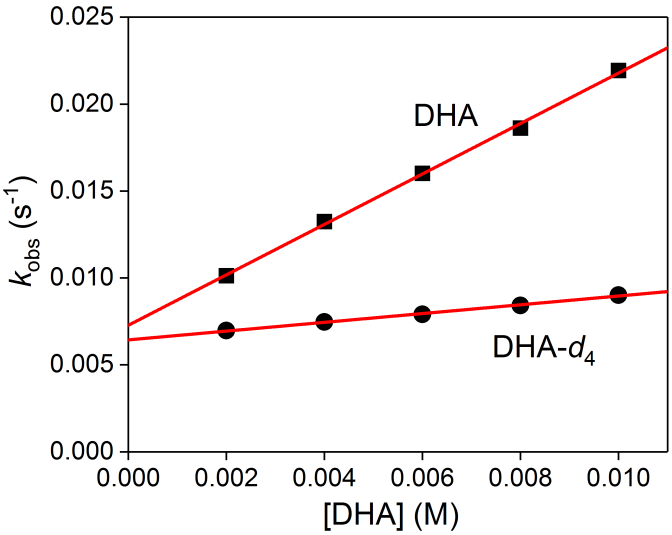

Figure S15. Plots of k_{obs} as a function of the concentration of (■) DHA and (•) DHA-d_4 obtained in MeOH at -60 °C, fitted linearly (red lines).

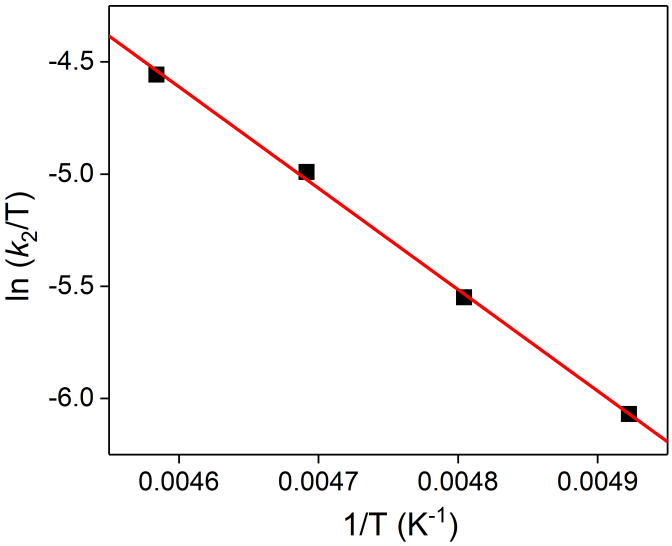

Figure S16. Eyring plot for DHA oxidation by **3**.

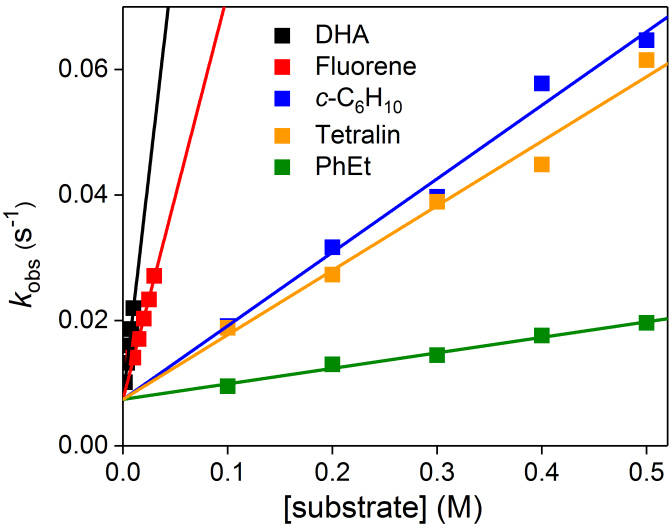

Figure S17. Plots of k_{obs} as a function of the substrate concentration for DHA, fluorene, cyclohexene, tetralin and ethylbenzene obtained in MeOH at -60 ^{o}C, fitted linearly.

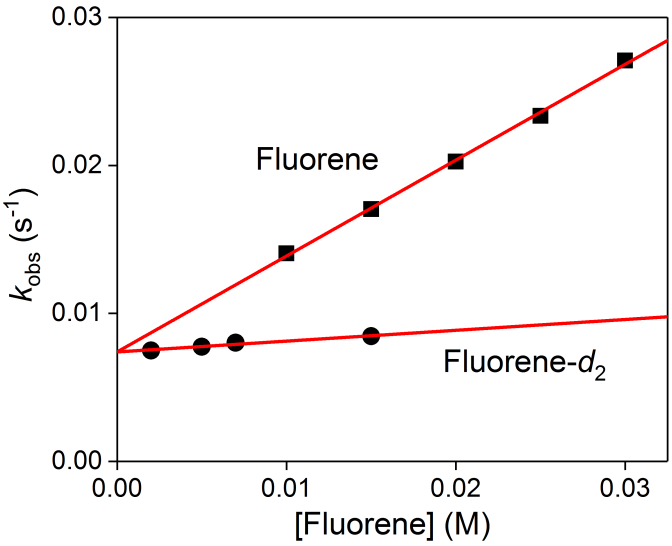

Figure S18. Plots of k_{obs} as a function of the concentration of (■) fluorene and (•) fluorene-d_2 obtained in MeOH at -60 ^{o}C, fitted linearly (red lines).

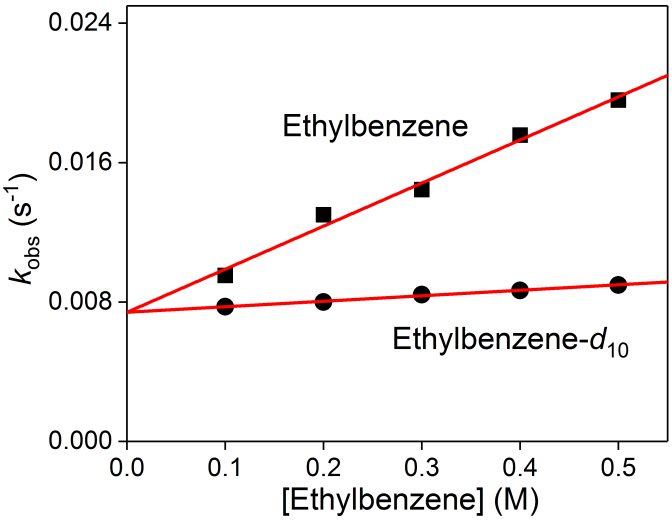

Figure S19. Plots of k_{obs} as a function of the concentration of (■) ethylbenzene and (•) ethylbenzene-d_2 obtained in MeOH at -60 ^{o}C, fitted linearly (red lines).

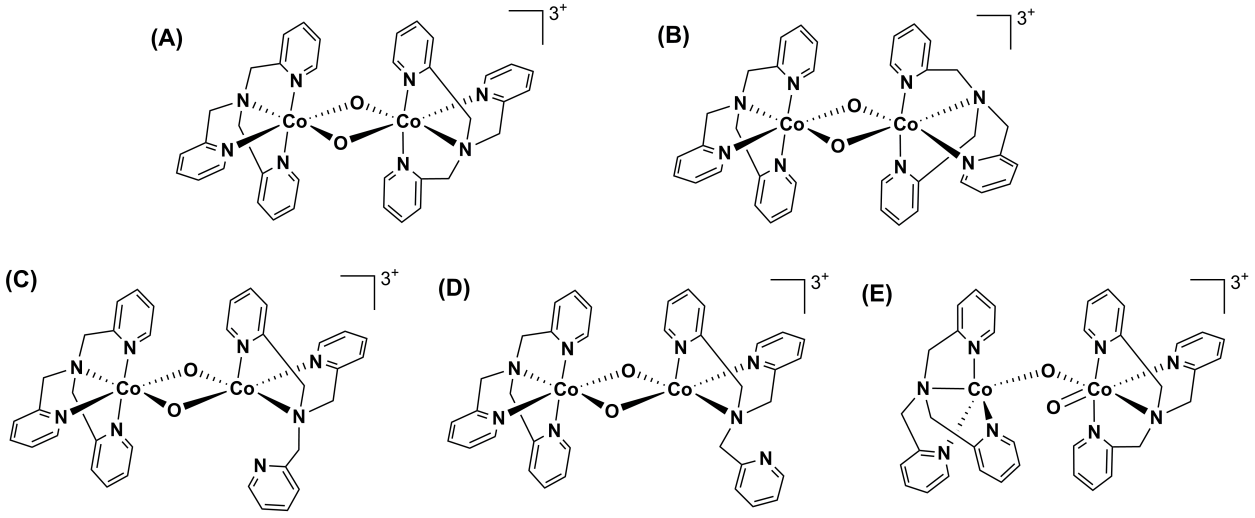

Scheme S1. Schematic representations of the structures of complex **3**, optimized at the BP86/6-31G(D) level of theory: (A) symmetric *trans*-diamond core, (B) symmetric *cis*-diamond core, (C) asymmetric arm-in diamond core, (D) asymmetric arm-out diamond core, and (E) asymmetric single μ-O open core.

Table S1. Selected EXAFS fits for **2**.[a]

	Co-N/O			Co···C			Co···Co					
Fit	**n**	**r**	**σ^2**	**n**	**r**	**σ^2**	**n**	**r**	**σ^2**	**ΔE_0**	**R-factor**	**red. χ^2**
1	4O	1.89	3.1							-5.39	0.0257	70.98
2	4N	1.91	2.0							-5.74	0.0152	42.09
3	5N	1.91	3.2							-6.56	0.0102	28.14
4	6N	1.91	4.2							-7.35	0.0252	69.55
5	4N 1N	1.89 1.94	3.5 0.1							-7.63	0.0088	44.01
6	1O 4N	1.84 1.84	9.9 2.2							-7.65	0.0107	53.59
7	5N	1.91	3.1							-6.51	0.0760	106.66
8	5N	1.91	3.1	4	2.82	4.7				-5.28	0.0199	35.09
9	5N	1.91	3.2	5	2.83	5.9				-5.10	0.0168	29.65
10	5N	1.91	3.2	6	2.83	7.0				-4.95	0.0153	26.99
11	5N	1.92	3.2	7	2.83	8.0				-4.83	0.0150	26.43
12	5N	1.91	3.2	4 3	2.78 2.92	1.3 0.2				-4.67	0.0101	23.93
13	5N	1.92	3.2	4 4	2.78 2.91	2.0 2.1				-4.54	0.0125	29.54
14	5N	1.92	3.2	4 5	2.77 2.91	2.8 4.2				-4.45	0.0152	36.03
15	5N	1.92	3.2	7 2	2.81 2.95	5.4 0.8				-4.52	0.0150	35.37
16	5N	1.91	3.1				1	2.80	7.3	-6.54	0.0266	46.77
17	**5N**	**1.91**	**3.1**	**4** **4**	**2.72** **2.94**	**8.0** **0.3**	**1**	**2.78**	**2.7**	**-5.24**	**0.0053**	**19.13**
18	5N	1.91	3.1	4 5	2.69 2.93	8.0 1.0	1	2.77	2.3	-5.18	0.0057	20.52
19	5N	1.91	3.1	7 3	2.75 2.94	19.9 0.1	1	2.78	3.6	-5.42	0.0057	20.42
20	5N	1.91	3.1	7 4	2.73 2.93	19.2 1.0	1	2.77	3.4	-5.42	0.0061	22.02

[a] Fitting range was k = 2.0-14.0 Å^{-1} (resolution = 0.13 Å) with back transform ranges of 1-2.0 Å for fits 1-6 and 1-2.7 Å for fits 7-20. r is in units of Å; σ^2 is in units of 10^{-3} Å; ΔE_0 is in units of eV; R represents the fractional mis-fit of the data, while χ^2 is the χ^2 fitting metric normalized by the number of independent data points in a given fit.

Table S2. Selected EXAFS fits for **3**.[a]

	Co-N/O			Co···C			Co···Co					
Fit	**n**	**r**	**σ^2**	**n**	**r**	**σ^2**	**n**	**r**	**σ^2**	**ΔE_0**	**R-factor**	**red. χ^2**
1	3O	1.90	0.6							-4.11	0.0333	26.18
2	4O	1.90	1.9							-5.05	0.0120	9.43
3	5O	1.90	3.0							-5.95	0.0218	17.17
4	4N	1.92	1.0							-5.97	0.0199	15.64
5	5N	1.92	2.0							-6.62	0.0038	3.01
6	6N	1.92	2.9							-7.25	0.0074	5.85
7	1O 4N	1.89 1.92	3.8 1.8							-6.48	0.0042	5.91
8	5N	1.92	1.9							-6.49	0.0641	25.60
9	5N	1.92	2.0	5	2.81	4.6				-5.53	0.0124	6.20
10	5N	1.92	2.0	6	2.81	5.7				-5.41	0.0120	6.01
11	5N	1.92	2.0	7	2.81	6.7				-5.30	0.0126	6.30
12	5N	1.92	2.0	5 3	2.78 2.92	1.9 1.0				-4.97	0.0104	7.03
13	5N	1.92	2.0	5 4	2.78 2.91	2.6 3.3				-4.86	0.0131	8.80
14	5N	1.92	2.0	6 3	2.79 2.93	3.2 2.0				-4.88	0.0131	8.79
15	5N	1.92	2.0	6 4	2.79 2.93	4.2 5.6				-4.79	0.0157	10.58
16	5N	1.92	1.9				1	2.78	5.9	-6.72	0.0166	8.33
17	5N	1.92	2.0	5	2.89	4.5	1	2.75	4.6	-4.79	0.0088	5.92
18	**5N**	**1.92**	**2.0**	**5**	**2.84**	**11.5**	**1**	**2.78**	**7.6**	**-5.47**	**0.0084**	**5.67**
19	5N	1.92	2.0	6	2.85	13.4	1	2.78	7.4	-5.35	0.0085	5.73
20	5N	1.92	2.0	7	2.85	15.6	1	2.78	7.2	-5.30	0.0088	5.94

[a] Fitting range was k = 2.0-14.0 Å^{-1} (resolution = 0.13 Å) with back transform ranges of 1-2.0 Å for fits 1-7 and 1-2.7 Å for fits 8-20. r is in units of Å; σ^2 is in units of 10^{-3} Å; ΔE_0 is in units of eV; R represents the fractional mis-fit of the data, while χ^2 is the χ^2 fitting metric normalized by the number of independent data points in a given fit.

Table S3. Summary of the metal-metal distances for selected diamond core and non-diamond core complexes.

Complex	M•••M	Method	Ref
Diamond core			
$[Fe^{III}_2(\mu\text{-}O)_2(6\text{-}Me_3\text{-}TPA)_2]^{2+}$	2.716	C.S.	16, 17
$[Fe^{III,IV}_2(\mu\text{-}O)_2(5\text{-}Et_3\text{-}TPA)_2]^{3+}$	2.683	C.S.	18
$[Fe^{IV}_2(\mu\text{-}O)_2(TPA^*)_2]^{4+}$	2.73	EXAFS	19
$[Mn^{III}_2(\mu\text{-}O)_2(TPA)_2]^{2+}$	2.656	C.S.	20
$[Mn^{III,IV}_2(\mu\text{-}O)_2(TPA)_2]^{3+}$	2.643	C.S.	21
$[Mn^{IV,IV}_2(\mu\text{-}O)_2(phen)_4]^{4+}$	2.748	C.S.	22
$Co^{III}_2(\mu\text{-}O)_2(L^{iPr})_2$	2.672	C.S.	23
$Co^{III}_2(\mu\text{-}O)_2(Me_2NN)_2$	2.716	C.S.	24
$Co^{III}_2(\mu\text{-}O)_2(Ar^{iPr8}O)_2$	2.721	C.S.	25
$Co^{III}_2(\mu\text{-}O)_2(Tp^{Me3})_2$	2.728	C.S.	26
$[Co^{III}_2(\mu\text{-}O)_2L_2]^{2-}$	2.737	C.S.	27
$L^{tBu}Co^{III}(\mu\text{-}O)_2Co^{III}L^{Me3}$	2.739	C.S.	28
$[Co^{III}_2(\mu\text{-}O)_2(TPA)_2]^{2+}$	2.78	EXAFS	This work
$[Co^{III,IV}_2(\mu\text{-}O)_2(TPA)_2]^{3+}$	2.78	EXAFS	This work
$Ni^{III}_2(\mu\text{-}O)_2(Tp^{Me3})_2$	2.882	C.S.	26
$[Ni^{III}_2(\mu\text{-}O)_2(Me_3\text{-}TPA)_2]^{2+}$	2.924	C.S.	29
$[Ni^{III}_2(\mu\text{-}O)_2(Me_2\text{-}TPA)_2]^{2+}$	2.796	C.S.	30
$[Cu^{III}_2(\mu\text{-}O)_2(6\text{-}Me_2\text{-}TPA)_2]^{2+}$	2.758	C.S.	31
Non-diamond core			
$[Co^{III}_2(\mu\text{-}OH)_2(TPA)_2]^{4+}$	2.944	C.S.	32
cis-$[Co^{III}_2(\mu\text{-}OH)(\mu\text{-}OO)(TPA)_2]^{3+}$	3.265	C.S.	33
trans-$[Co^{III}_2(\mu\text{-}OH)(\mu\text{-}OO)(TPA)_2]^{3+}$	3.256	C.S.	34
$[Cu^{II}_2(\mu\text{-}\eta^2\text{:}\eta^2(O_2))(MeAN)_2]^{2+}$	3.533	C.S.	35

C.S.: crystal structure
TPA: tris(2-pyridylmethyl)amine
TPA*: tris(3,5-dimethyl-4-methoxy-2-pyridylmethyl)amine
6-Me_3-TPA: tris(6-methyl-2-pyridylmethyl)amine
5-Et_3-TPA: tris(5-ethyl-2-pyridylmethyl)amine
phen: 1,10-phenanthroline
L^{iPr}: 1,3-bis(2,6-diisopropyl-phenylimino)propyl
L^{tBu}: 2,2,6,6-tetramethyl-3,5-bis(2,6-diisopropyl-phenylimino)heptyl
L^{Me3}: 2,4-bis(2,6-dimethyl-phenylimino)-3-methylpentyl
Me_2NN: 2,4-bis(2,6-dimethyl-phenylimino)pentyl
Ar^{iPr8}: C_6H-2,6-(C_6H_2-2,4,6-$^iPr_3$)$_2$-3,5-iPr_2
Tp^{Me3}: hydrotris(3,4,5-trimethyl-1-pyrazolyl)borate
MeAN: *N*-methyl-*N,N*-bis[3-(dimethylamino)propyl]-amine

Table S4. Detailed BP86/6-31G(D) geometry optimized structures for **2** and **3** (see Scheme S1 for a schematic illustration of structures).

Complex	Structure	Multiplicity	Relative Energy (kJ/mol)	Co•••Co distance (Å)
2	***Trans***	**singlet**	**0.00**	**2.78**
	Cis	singlet	31.15	2.80
	Trans	triplet	115.39	2.76
	Cis[a]	triplet	133.46	2.73
	N arm-in	singlet	61.25	2.74
	N arm-out	singlet	35.50	2.74
3	***Trans***	**doublet**	**0.00**	**2.77**
	Cis	doublet	27.41	2.78
	Trans	quadruplet	115.90	2.73
	Cis	quadruplet	128.79	2.74
	N arm-in	doublet	96.39	2.70
	N arm-out	doublet	75.22	2.71
	μ-O	doublet	187.49	3.40

[a]Here one of the Co-N bonds is unusually long.

Table S5. Spin density distribution of **3**.

Method/basis set	Spin density			
	Co1	Co2	O1	O2
BP86/6-31G(D)	0.27	0.27	0.22	0.22
M06-l/6-31G(D)	0.23	0.23	0.27	0.27
B3LYP/6-31G(D)	0.18	0.18	-0.01	0.63
B3LYP*(15% HF)/6-31G(D)	0.24	0.24	0.25	0.25

Table S6. Co-O and Co-N distances in BP86/6-31G(D) geometry optimized *trans*- structures of **2** and **3** in methanol.

	r(Co-O) (Å)	*r*(Co-N) (Å)
2	1.848, 1.866	1.918, 1.921, 1.939, 2.002
3	1.816, 1.836	1.936, 1.937, 1.946, 2.000

Table S7. Optimized structures of **2** and **3** obtained using various DFT methods in combination with the polarized continuum model with methanol parameters.

Complex	Functional/Basis set	Configuration	Multiplicity	Electronic Energy (kJ/mol)	***R*(Co•••Co) (Å)**
2	B3LYP/6-31G(d)	*trans*	singlet	-12,463,685.33	2.76
	B3LYP/6-31G(d)	*cis*	singlet	-12,463,654.83	2.78
	B3LYP/6-31G(d)	*trans*	triplet	-12,463,672.27	2.74
	B3LYP/6-31G(d)	*cis*	triplet	-12,463,682.68[a]	2.72
	B3LYP*(15%HF)/6-31G(d)	*trans*	singlet	-12,294,115.37	2.88
	B3LYP*(15%HF)/6-31G(d)	*cis*	singlet	-12,294,084.99	2.90
	B3LYP*(15%HF)/6-31G(d)	*trans*	triplet	-12,294,099.13	2.84
	B3LYP*(15%HF)/6-31G(d)	*cis*	triplet	-12,294,123.24[b]	2.82
	M06-L/6-31G(d)	*trans*	singlet	-12,462,824.34	2.73
	M06-L/6-31G(d)	*cis*	singlet	-12,462,781.85	2.74
	M06-L/6-31G(d)	*trans*	triplet	-12,462,779.03	2.71
	M06-L/6-31G(d)	*cis*	triplet	-12,462,753.22[c]	2.71
3	B3LYP/6-31G(d)	*trans*	doublet	-12,463,232.25	2.76
	B3LYP/6-31G(d)	*cis*	doublet	-12,463,208.67	2.78
	B3LYP/6-31G(d)	*trans*	quadruplet	-12,463,214.43	2.73
	B3LYP/6-31G(d)	*cis*	quadruplet	-12,463,199.46	2.74
	B3LYP*(15%HF)/6-31G(d)	*trans*	doublet	-12,293,816.05	2.86
	B3LYP*(15%HF)/6-31G(d)	*cis*	doublet	-12,293,789.10	2.87
	B3LYP*(15%HF)/6-31G(d)	*trans*	quadruplet	-12,293,797.27	2.83
	B3LYP*(15%HF)/6-31G(d)	*cis*	quadruplet	-12,293,782.52	2.83
	M06-L/6-31G(d)	*trans*	doublet	-12,462,394.78	2.73
	M06-L/6-31G(d)	*cis*	doublet	-12,462,358.20	2.74
	M06-L/6-31G(d)	*trans*	quadruplet	-12,462,362.09	2.70
	M06-L/6-31G(d)	*cis*	quadruplet	-12,462,338.21	2.71

[a] Triplet state was more stable than the singlet state, which could be attributed to the tendency of the B3LYP functional to overstabilize high-spin states.[13]

[b] Geometry optimization has led to the opening of one of the Co-N bonds.

[c] One small imaginary frequency of 4.43*i* cm^{-1} was present likely due to the numerical noise.

Table S8. Kinetic and product analysis results for the reaction of **3** with substrates.

Substrate	k_2 (M^{-1} s^{-1})	Product(s) and yield under air	Product(s) and yield under Ar
DHA	1.5(1)	Anthraquinone, 13 % Anthrone, trace Anthracene, trace	Anthraquinone, 19 % Anthrone, trace Anthracene, trace
DHA-d_4	0.25(1)	N.D	N.D.
Fluorene	0.65(2)	9-fluoreone, 26%	9-fluoreone, 27 %
Fluorene-d_2	0.074(1)	N.D.	N.D.
Cyclohexene	0.12(1)	2-cyclohexen-1-one, 28% 2-cyclohexen-1-ol, 10%	2-cyclohexen-1-one, 28% 2-cyclohexen-1-ol, 2%
Tetralin	0.10(1)	α-tetralone, 17% 1,2,3,4-tetrahydro-1-naphthol, 5%	α-tetralone, 23% 1,2,3,4-tetrahydro-1-naphthol, 9%
PhEt	0.025(2)	Acetophenone, 12%	Acetophenone, 15%
PhEt-d_{10}	0.0032(2)	N.D.	N.D.

N.D.: not determined.

Table S9. Summary of rate constants of DHA oxidation for selected dinuclear and mononuclear metal-oxo complexes.

Complex	k_2 (M^{-1} s^{-1})	Temp (^oC)	Ref
3	2.3	-55	This work
	1.5	-60	
	0.81	-65	
	0.47	-70	
$[Fe^{III,IV}_2(\mu\text{-}O)_2(5\text{-}Me_3\text{-}TPA)_2]^{3+}$	0.028 (with 0.05 M H_2O)	-30	36
	0.80 (with 1.0 M H_2O)	-30	36
$[Fe^{III,IV}_2(\mu\text{-}O)_2(TPA^*)_2]^{3+}$	10^{-5}	-30	19, 36
	0.15 (with 1.0 M H_2O)	-30	36
$[Fe^{IV}_2(\mu\text{-}O)_2(TPA^*)_2]^{4+}$	10^{-4}	-30	19, 36
$[(phen)_2Mn^{III}(\mu\text{-}O)_2Mn^{IV}(phen)_2]^{3+}$	0.0012	32	37
$[(phen)_2Mn^{III}(O)(OH)Mn^{III}(phen)_2]^{3+}$	0.00042	25	38
$[Cu^{III}_2(\mu\text{-}O)_2]^{2+}$	0.22	-70	39
$[HO\text{-}Fe^{III}\text{-}O\text{-}Fe^{IV}{=}O]^{2+}$	28	-80	36, 40
$[HO\text{-}Fe^{IV}\text{-}O\text{-}Fe^{IV}{=}O]^{3+}$	0.027	-80	40
$[D_3CO\text{-}Fe^{III}\text{-}O\text{-}Fe^{IV}{=}O]^{2+}$	360	-80	36, 40
$[(TAML)Co^{IV}(O)(Sc)]^{+}$	0.21	5	41
$[(13\text{-}TMC)Co^{IV}(O)]^{2+}$	0.083	-40	42

TPA*: tris(3,5-dimethyl-4-methoxy-2-pyridylmethyl)amine
5-Me_3-TPA: tris(5-methyl-2-pyridylmethyl)amine
phen: 1,10-phenanthroline
TAML: tetraamido macrocyclic ligand
13-TMC: 1,4,7,10-tetramethyl-1,4,7,10-tetraazacyclotridecane

Table S10. Cartesian coordinates for optimized *cis*-**2** complex.

Co	-1.73948	-0.47535	0.70792
N	-3.22399	-1.25729	1.80522
C	-2.95830	-0.74207	3.18902
H	-2.06514	-1.27672	3.55145
H	-3.80485	-0.92912	3.87381
N	-1.93908	1.01355	1.91474
C	-2.63701	0.72543	3.05264
C	-3.04049	1.72820	3.93925
H	-3.60284	1.46128	4.83882
C	-2.73646	3.06672	3.63908
H	-3.04884	3.86881	4.31471
C	-2.06128	3.35798	2.44537
H	-1.83340	4.38776	2.15646
C	-1.68186	2.30396	1.60607
H	-1.16601	2.45233	0.65457
C	-4.56105	-0.81113	1.26932
H	-5.11730	-0.28700	2.06617
H	-5.16261	-1.69782	1.00250
N	-3.14170	0.36471	-0.34209
C	-4.41380	0.09783	0.06116
C	-5.51888	0.63929	-0.60923
H	-6.53138	0.40954	-0.26289
C	-5.30675	1.47066	-1.71848
H	-6.15750	1.90168	-2.25494
C	-3.99012	1.73999	-2.12743
H	-3.78066	2.38292	-2.98686
C	-2.93362	1.16939	-1.41409
H	-1.88148	1.33200	-1.67050
C	-3.02244	-2.73775	1.69244
H	-3.88463	-3.30659	2.08381
H	-2.12497	-2.97502	2.28656
N	-2.04610	-2.04540	-0.38984
C	-2.75038	-3.03305	0.23818
C	-3.20491	-4.16315	-0.44846
H	-3.76868	-4.93192	0.08819
C	-2.94849	-4.27449	-1.82496
H	-3.29873	-5.14759	-2.38392
C	-2.27203	-3.23216	-2.47369
H	-2.08082	-3.25932	-3.54997
C	-1.84144	-2.13209	-1.72272
H	-1.32665	-1.27922	-2.16923
O	-0.22207	0.17834	-0.16628
O	-0.46526	-1.32454	1.73923
H	2.32143	-5.36025	-2.29772
C	2.01910	-4.48055	-1.72138
H	2.50256	-5.35220	0.22075
C	2.11406	-4.48402	-0.31967
H	1.50971	-3.26244	-3.45812
C	1.56767	-3.32104	-2.36768

C	1.72711	-3.34299	0.38973
C	1.19382	-2.21557	-1.59484
H	2.55800	-3.87242	2.33978
C	1.84590	-3.16228	1.88272
N	1.24319	-2.23460	-0.24441
H	0.85337	-3.28962	2.34520
H	0.84795	-1.27361	-2.02626
H	4.18762	-2.42941	1.54188
N	2.24192	-1.73510	2.11696
C	3.68922	-1.47393	1.78252
Co	1.04825	-0.68870	0.89231
C	3.83816	-0.50750	0.61993
C	5.08955	-0.10775	0.13184
H	6.00282	-0.49720	0.59243
N	2.68365	-0.04221	0.07029
H	0.85953	-1.64819	3.68630
C	1.86723	-1.24905	3.48452
C	5.15000	0.79058	-0.94339
H	4.20313	-1.07084	2.67286
C	2.73904	0.82612	-0.97033
H	2.57017	-1.60212	4.26006
C	3.95265	1.26571	-1.50374
H	6.11810	1.11478	-1.33722
H	1.76503	1.15036	-1.35184
H	3.95490	1.96693	-2.34289
C	1.79574	0.25582	3.40738
N	1.32487	0.70903	2.20779
C	1.31878	2.03823	1.96488
C	2.21066	1.13367	4.41343
H	0.98683	2.32511	0.96510
H	2.58680	0.73392	5.35974
C	1.72216	2.97379	2.92493
C	2.15829	2.51729	4.17645
H	1.69728	4.04006	2.68375
H	2.48172	3.22294	4.94771

Table S11. Cartesian coordinates for optimized *trans*-**2** complex.

Co	-1.73465	-0.50453	0.75543
N	-3.23083	-1.33182	1.79790
C	-3.00218	-0.84435	3.19720
H	-2.11942	-1.38590	3.57639
H	-3.86544	-1.04528	3.85655
N	-1.94450	0.94388	1.99495
C	-2.67186	0.62799	3.10574
C	-3.05687	1.60713	4.02684
H	-3.64459	1.32523	4.90550
C	-2.69130	2.94343	3.79203
H	-2.98758	3.72702	4.49613
C	-1.96232	3.25931	2.63574
H	-1.67161	4.28913	2.41043
C	-1.60827	2.23070	1.75531
H	-1.03088	2.38412	0.83871
C	-4.56602	-0.88806	1.25240
H	-5.13120	-0.37438	2.04964
H	-5.16138	-1.77448	0.97138
N	-3.12987	0.32730	-0.30251
C	-4.40750	0.03523	0.05906
C	-5.50143	0.56914	-0.63538
H	-6.51992	0.31861	-0.32280
C	-5.26904	1.42054	-1.72516
H	-6.11006	1.84672	-2.28059
C	-3.94503	1.71611	-2.09064
H	-3.72087	2.37516	-2.93407
C	-2.90081	1.15055	-1.35560
H	-1.84207	1.32708	-1.57309
C	-3.00879	-2.80448	1.63342
H	-3.87417	-3.39943	1.97572
H	-2.12733	-3.05736	2.24649
N	-1.93995	-2.04281	-0.37712
C	-2.67684	-3.04771	0.17919
C	-3.06678	-4.16510	-0.56593
H	-3.66154	-4.95255	-0.09368
C	-2.69503	-4.24445	-1.91857
H	-2.99400	-5.10683	-2.52229
C	-1.95502	-3.19599	-2.48558
H	-1.65764	-3.21368	-3.53772
C	-1.59757	-2.10668	-1.68290
H	-1.01392	-1.25375	-2.04125
O	-0.28976	0.21931	-0.14169
O	-0.40015	-1.31395	1.77896
H	2.30414	4.01213	4.15966
C	2.00515	3.14977	3.55592
H	2.97170	3.85788	1.73105
C	2.37691	3.07044	2.20328
H	0.96771	2.11900	5.17504
C	1.26510	2.10133	4.12291

C	1.98695	1.95306	1.45814
C	0.90764	1.01204	3.32020
H	3.18430	2.30481	-0.33839
C	2.31890	1.70986	0.00390
N	1.25004	0.94818	2.01442
H	1.43746	1.96277	-0.60916
H	0.32397	0.15911	3.67854
H	4.47156	0.67980	0.66575
N	2.54092	0.23720	-0.16061
C	3.87611	-0.20660	0.38485
Co	1.04474	-0.59009	0.88186
C	3.71760	-1.12979	1.57827
C	4.81152	-1.66361	2.27279
H	5.83001	-1.41304	1.96023
N	2.43996	-1.42190	1.93982
H	1.42948	0.29132	-1.93908
C	2.31225	-0.25023	-1.55992
C	4.57914	-2.51496	3.36260
H	4.44120	-0.72040	-0.41238
C	2.21090	-2.24510	2.99294
H	3.17550	-0.04929	-2.21928
C	3.25512	-2.81058	3.72805
H	5.42016	-2.94106	3.91809
H	1.15216	-2.42167	3.21041
H	3.03096	-3.46959	4.57150
C	1.98193	-1.72258	-1.46848
N	1.25460	-2.03849	-0.35767
C	0.91839	-3.32532	-0.11805
C	2.36692	-2.70170	-2.38961
H	0.34102	-3.47875	0.79857
H	2.95461	-2.41978	-3.26828
C	1.27242	-4.35391	-0.99850
C	2.00136	-4.03800	-2.15481
H	0.98173	-5.38373	-0.77319
H	2.29764	-4.82158	-2.85893

Table S12. Cartesian coordinates for optimized N-arm out **2** complex.

Co	-1.60902	-0.45842	0.62494
N	-2.78173	-1.47531	1.87523
C	-2.41796	-0.98059	3.24333
H	-1.47482	-1.47839	3.52620
H	-3.18579	-1.24178	3.99245
N	-1.66475	0.91983	1.96719
C	-2.16519	0.50739	3.16641
C	-2.35295	1.40250	4.22475
H	-2.76489	1.04468	5.17270
C	-2.00454	2.75058	4.04576
H	-2.14336	3.46807	4.86012
C	-1.48569	3.16334	2.80993
H	-1.20598	4.20457	2.62822
C	-1.33453	2.21849	1.78882
H	-0.93585	2.46398	0.80137
C	-4.23683	-1.23266	1.54472
H	-4.77977	-0.92972	2.45645
H	-4.68932	-2.18343	1.21239
N	-3.24642	0.24612	-0.11758
C	-4.39757	-0.19039	0.45725
C	-5.64715	0.28508	0.03773
H	-6.55919	-0.08140	0.51839
C	-5.70393	1.22657	-0.99943
H	-6.66966	1.61080	-1.34162
C	-4.50843	1.66764	-1.59004
H	-4.51064	2.39996	-2.40196
C	-3.29629	1.15657	-1.12099
H	-2.32204	1.44947	-1.52481
C	-2.39236	-2.90754	1.64941
H	-3.11554	-3.61010	2.09918
H	-1.40962	-3.04975	2.12986
N	-1.76064	-2.00822	-0.48920
C	-2.23076	-3.11194	0.16170
C	-2.49152	-4.30406	-0.52040
H	-2.87699	-5.16927	0.02660
C	-2.25489	-4.36219	-1.90349
H	-2.45399	-5.28424	-2.45789
C	-1.77310	-3.22189	-2.56262
H	-1.58330	-3.22390	-3.63923
C	-1.54102	-2.05701	-1.82248
H	-1.16488	-1.13043	-2.26421
H	5.69883	0.07914	3.72741
C	4.83404	-0.03073	3.06599
H	3.61256	-1.13180	4.50175
H	5.74368	1.02876	1.39152
C	3.67859	-0.70054	3.49888
C	4.86190	0.50131	1.76780
C	2.58896	-0.80442	2.63122
C	3.74314	0.34756	0.94125

H	1.64711	-1.29053	2.90268
N	2.61573	-0.28901	1.37417
H	4.24727	1.75566	-0.64419
C	3.70595	0.80392	-0.49736
H	4.20287	0.04396	-1.12663
H	0.72841	2.35010	-1.06386
N	2.27806	0.95040	-0.96395
Co	1.08883	-0.21876	0.19903
C	1.81910	2.38553	-0.91506
H	2.02196	2.73686	0.11089
H	2.81915	0.72048	-3.05951
N	1.71273	-1.57808	-0.94212
C	2.08546	0.34826	-2.32249
H	1.33686	-3.17071	0.33966
C	1.70016	-2.90573	-0.65544
C	2.14955	-1.15135	-2.16516
C	2.47936	3.31675	-1.91826
C	2.12432	-3.85582	-1.58840
C	2.59339	-2.05436	-3.13467
C	2.57521	-3.42901	-2.84732
N	3.73468	3.73914	-1.62023
H	2.10194	-4.91587	-1.32136
H	2.95072	-1.67961	-4.09834
H	2.91812	-4.15305	-3.59225
H	1.07431	0.64162	-2.65734
H	0.78611	3.36574	-3.28335
C	1.80300	3.72044	-3.08527
C	4.34200	4.56737	-2.49444
H	5.35673	4.88749	-2.22505
C	2.44527	4.59086	-3.97901
C	3.74409	5.02477	-3.67995
H	1.93769	4.92474	-4.89005
H	4.28506	5.70581	-4.34414
O	-0.42875	0.43640	-0.47714
O	-0.00585	-1.06728	1.33457

Table S13. Cartesian coordinates for optimized N-arm in **2** complex.

Co	-1.34464	-0.45893	0.51210
N	-2.73613	-1.38169	1.60951
C	-2.48171	-0.94768	3.01999
H	-1.62745	-1.53948	3.39108
H	-3.34849	-1.14530	3.67464
N	-1.39895	0.89068	1.89420
C	-2.07619	0.50772	3.01460
C	-2.28178	1.38742	4.08231
H	-2.83946	1.05314	4.96200
C	-1.75544	2.68643	4.00323
H	-1.90424	3.39248	4.82602
C	-1.03817	3.06015	2.85841
H	-0.60416	4.05911	2.75981
C	-0.88091	2.13777	1.81562
H	-0.31730	2.37161	0.90300
C	-4.11977	-1.00133	1.13408
H	-4.72644	-0.66203	1.99126
H	-4.61947	-1.90118	0.73437
N	-2.82691	0.40623	-0.37399
C	-4.06820	0.06682	0.06217
C	-5.21777	0.65929	-0.47692
H	-6.20536	0.37065	-0.10469
C	-5.07850	1.61614	-1.49206
H	-5.96377	2.09046	-1.92645
C	-3.79139	1.95517	-1.94003
H	-3.63914	2.69662	-2.72899
C	-2.68701	1.33103	-1.35565
H	-1.65298	1.54388	-1.64433
C	-2.45441	-2.83960	1.38813
H	-3.28158	-3.47959	1.74203
H	-1.54603	-3.08085	1.96597
N	-1.52401	-1.96794	-0.64993
C	-2.15504	-3.03481	-0.07920
C	-2.44926	-4.18687	-0.81463
H	-2.96509	-5.02211	-0.33224
C	-2.07637	-4.24387	-2.16730
H	-2.29762	-5.13506	-2.76233
C	-1.43135	-3.14058	-2.74499
H	-1.13339	-3.14173	-3.79687
C	-1.17511	-2.01383	-1.95551
H	-0.67777	-1.11632	-2.33319
H	5.44917	-0.01271	4.51601
C	4.68357	-0.14781	3.74604
H	3.15161	-0.89921	5.10613
H	5.94096	0.54951	2.10459
C	3.41018	-0.63705	4.07625
C	4.96011	0.16998	2.40629
C	2.45143	-0.77823	3.06918
C	3.96171	-0.01244	1.44551

H	1.43290	-1.13384	3.24994
N	2.71842	-0.47083	1.77271
H	4.95176	0.92629	-0.24988
C	4.15973	0.18827	-0.03463
H	4.48730	-0.76963	-0.47568
H	2.85046	2.46371	0.26200
N	2.85670	0.58673	-0.69259
Co	1.38611	-0.39705	0.37955
C	2.85127	2.09992	-0.77807
H	3.80928	2.40317	-1.24547
H	3.60325	0.16427	-2.68940
N	1.99674	-1.86762	-0.62508
C	2.74189	-0.06713	-2.03459
H	1.29714	-3.33881	0.66041
C	1.79367	-3.17085	-0.29731
C	2.59678	-1.55359	-1.81247
C	1.72464	2.78609	-1.53133
C	2.18817	-4.20621	-1.14886
C	3.01999	-2.54638	-2.69996
C	2.80805	-3.89481	-2.36907
N	0.76882	3.37930	-0.77822
H	2.01112	-5.24278	-0.84908
H	3.51294	-2.26120	-3.63398
H	3.13179	-4.68764	-3.04977
H	1.82655	0.32903	-2.50657
C	1.76321	2.91752	-2.93495
C	-0.18359	4.09215	-1.41448
C	0.75846	3.64966	-3.58358
C	-0.24143	4.25234	-2.80799
O	0.00560	0.32452	-0.46479
O	0.12049	-1.21003	1.36301
H	-1.03827	4.84728	-3.26472
H	-0.93713	4.56330	-0.77041
H	0.76999	3.76149	-4.67267
H	2.58154	2.47395	-3.51167

Table S14. Cartesian coordinates for optimized *cis*-**3** complex.

Co	-1.72999	-0.47402	0.70745
N	-3.21460	-1.25678	1.79515
C	-2.96540	-0.75681	3.18932
H	-2.08737	-1.30107	3.57605
H	-3.82641	-0.95041	3.85210
N	-1.96647	1.02032	1.92667
C	-2.64326	0.70970	3.06996
C	-3.01947	1.69880	3.98353
H	-3.56452	1.41884	4.88912
C	-2.71263	3.03853	3.70005
H	-3.00519	3.82965	4.39656
C	-2.05930	3.35061	2.49940
H	-1.82945	4.38335	2.22545
C	-1.70236	2.31268	1.63283
H	-1.20894	2.48807	0.67479
C	-4.54921	-0.79544	1.25123
H	-5.10039	-0.26667	2.04755
H	-5.15664	-1.67710	0.98365
N	-3.12351	0.38049	-0.35573
C	-4.39300	0.11261	0.04601
C	-5.49305	0.65914	-0.62900
H	-6.50786	0.43289	-0.28896
C	-5.26917	1.49066	-1.73439
H	-6.11562	1.92554	-2.27408
C	-3.95152	1.75823	-2.13934
H	-3.73667	2.40146	-2.99644
C	-2.89936	1.18384	-1.42339
H	-1.84750	1.34606	-1.67909
C	-3.03238	-2.74140	1.67933
H	-3.90923	-3.29090	2.06176
H	-2.15251	-3.00911	2.28786
N	-2.06517	-2.04066	-0.40349
C	-2.75649	-3.03351	0.22789
C	-3.18608	-4.17294	-0.45898
H	-3.74151	-4.94845	0.07543
C	-2.91603	-4.28225	-1.83152
H	-3.24733	-5.16245	-2.39018
C	-2.24979	-3.23360	-2.48076
H	-2.04834	-3.26202	-3.55450
C	-1.84279	-2.12349	-1.73388
H	-1.34343	-1.26555	-2.18735
O	-0.22618	0.16298	-0.14608
O	-0.46167	-1.29814	1.70723
H	2.27086	-5.42075	-2.24918
C	1.99045	-4.52603	-1.68575
H	2.46502	-5.37767	0.26650
C	2.09254	-4.51111	-0.28641
H	1.49586	-3.32674	-3.44090
C	1.55934	-3.36940	-2.35072

C	1.73328	-3.35150	0.40699
C	1.21181	-2.24384	-1.59696
H	2.57601	-3.84605	2.35887
C	1.85072	-3.15579	1.89531
N	1.27031	-2.24694	-0.24671
H	0.86554	-3.30439	2.36841
H	0.89175	-1.30614	-2.05489
H	4.18236	-2.40639	1.53331
N	2.23270	-1.72100	2.11334
C	3.68075	-1.45147	1.76613
Co	1.03762	-0.68464	0.88996
C	3.82019	-0.49541	0.59649
C	5.06812	-0.09979	0.09571
H	5.98473	-0.48723	0.55001
N	2.66839	-0.02861	0.04912
H	0.87531	-1.64338	3.72059
C	1.87408	-1.23712	3.48781
C	5.11689	0.79172	-0.98421
H	4.19347	-1.03627	2.65079
C	2.70755	0.83385	-0.99498
H	2.59242	-1.59308	4.24592
C	3.91800	1.26779	-1.53914
H	6.08186	1.11204	-1.38814
H	1.73388	1.16041	-1.37404
H	3.91513	1.96412	-2.38158
C	1.80159	0.26517	3.41036
N	1.34591	0.72098	2.20717
C	1.32309	2.04957	1.96125
C	2.19128	1.14646	4.42319
H	1.00792	2.34306	0.95838
H	2.55786	0.74986	5.37388
C	1.70208	2.98459	2.92991
C	2.12675	2.52786	4.18530
H	1.66751	4.05040	2.69069
H	2.43134	3.23552	4.96184

Table S15. Cartesian coordinates for optimized *trans*-**3** complex.

Co	-1.72741	-0.50452	0.75829
N	-3.22367	-1.32871	1.79800
C	-3.00997	-0.85329	3.20534
H	-2.13816	-1.40001	3.60402
H	-3.88396	-1.06443	3.84504
N	-1.97611	0.95230	2.00836
C	-2.68748	0.61809	3.12393
C	-3.06129	1.58580	4.06110
H	-3.63607	1.29138	4.94344
C	-2.70259	2.92401	3.83566
H	-2.99002	3.69826	4.55298
C	-1.99149	3.25731	2.67355
H	-1.70682	4.28947	2.45465
C	-1.64583	2.24255	1.77554
H	-1.09193	2.42941	0.85257
C	-4.55692	-0.87057	1.24485
H	-5.11525	-0.34807	2.04021
H	-5.15918	-1.75275	0.96793
N	-3.11633	0.33839	-0.31346
C	-4.39083	0.04600	0.05015
C	-5.48172	0.57997	-0.64914
H	-6.50121	0.33271	-0.33923
C	-5.24181	1.42643	-1.73968
H	-6.08033	1.85212	-2.29874
C	-3.91805	1.72018	-2.10503
H	-3.69075	2.37546	-2.94974
C	-2.87600	1.15591	-1.36674
H	-1.81957	1.33443	-1.58985
C	-3.02515	-2.80708	1.64205
H	-3.90666	-3.37668	1.98176
H	-2.16167	-3.08691	2.26943
N	-1.97034	-2.05346	-0.37947
C	-2.69475	-3.05814	0.19233
C	-3.07136	-4.18802	-0.54025
H	-3.65588	-4.97599	-0.05758
C	-2.70001	-4.27693	-1.89079
H	-2.98805	-5.14978	-2.48393
C	-1.97417	-3.22706	-2.47262
H	-1.67830	-3.25139	-3.52433
C	-1.62801	-2.12416	-1.68567
H	-1.06431	-1.27253	-2.07354
O	-0.29453	0.19472	-0.11087
O	-0.39538	-1.28931	1.74818
H	2.29814	4.05518	4.12124
C	2.01010	3.18234	3.52810
H	2.96597	3.88139	1.69488
C	2.38145	3.09343	2.17755
H	0.98839	2.15680	5.16164
C	1.28426	2.13247	4.10993

C	2.00484	1.96354	1.44498
C	0.93810	1.02957	3.32297
H	3.21675	2.28209	-0.34445
C	2.33525	1.71249	-0.00474
N	1.28044	0.95886	2.01678
H	1.47177	1.99232	-0.63212
H	0.37440	0.17794	3.71084
H	4.46927	0.65816	0.66937
N	2.53376	0.23411	-0.16069
C	3.86702	-0.22402	0.39245
Co	1.03750	-0.59008	0.87902
C	3.70092	-1.14059	1.58716
C	4.79181	-1.67456	2.28645
H	5.81131	-1.42730	1.97654
N	2.42642	-1.43298	1.95077
H	1.44826	0.30542	-1.96672
C	2.32007	-0.24130	-1.56804
C	4.55190	-2.52101	3.37699
H	4.42534	-0.74653	-0.40291
C	2.18609	-2.25050	3.00405
H	3.19405	-0.03017	-2.20773
C	3.22815	-2.81476	3.74234
H	5.39042	-2.94670	3.93606
H	1.12967	-2.42903	3.22716
H	3.00084	-3.47004	4.58705
C	1.99757	-1.71269	-1.48663
N	1.28620	-2.04690	-0.37105
C	0.95593	-3.33714	-0.13823
C	2.37138	-2.68039	-2.42380
H	0.40203	-3.52401	0.78474
H	2.94617	-2.38598	-3.30614
C	1.30159	-4.35191	-1.03624
C	2.01269	-4.01861	-2.19835
H	1.01692	-5.38407	-0.81734
H	2.30011	-4.79285	-2.91567

Table S16. Cartesian coordinates for optimized N-arm out **3** complex.

Co	-1.60904	-0.47467	0.58966
N	-2.74627	-1.46208	1.87635
C	-2.34017	-0.95746	3.23430
H	-1.39359	-1.45761	3.50168
H	-3.09149	-1.21572	3.99940
N	-1.63549	0.93656	1.91783
C	-2.09515	0.52867	3.13569
C	-2.25653	1.43581	4.18728
H	-2.63503	1.08666	5.15167
C	-1.92831	2.78415	3.97899
H	-2.04822	3.51009	4.78840
C	-1.45777	3.18973	2.72202
H	-1.19923	4.23157	2.51701
C	-1.32944	2.23627	1.70704
H	-0.97951	2.48900	0.70399
C	-4.21273	-1.20827	1.58766
H	-4.71615	-0.87769	2.51147
H	-4.68708	-2.16037	1.29385
N	-3.25972	0.23935	-0.12108
C	-4.39541	-0.18949	0.48634
C	-5.65217	0.27926	0.08231
H	-6.55438	-0.08041	0.58492
C	-5.72639	1.20362	-0.96784
H	-6.69835	1.58152	-1.29837
C	-4.54405	1.63691	-1.58902
H	-4.56137	2.35556	-2.41216
C	-3.32281	1.13366	-1.13765
H	-2.36277	1.42424	-1.57362
C	-2.38366	-2.90713	1.66055
H	-3.11258	-3.58259	2.13894
H	-1.39789	-3.07153	2.12742
N	-1.82418	-2.04197	-0.51661
C	-2.27077	-3.13266	0.17279
C	-2.55505	-4.33406	-0.48213
H	-2.91770	-5.19089	0.09221
C	-2.37139	-4.41061	-1.87157
H	-2.58822	-5.34127	-2.40386
C	-1.92483	-3.27882	-2.56869
H	-1.78374	-3.29414	-3.65217
C	-1.66624	-2.10221	-1.85793
H	-1.33107	-1.18160	-2.34203
H	5.66211	-0.01342	3.71084
C	4.79765	-0.10186	3.04618
H	3.58824	-1.26924	4.44053
H	5.70146	1.03299	1.41954
C	3.64983	-0.79862	3.45602
C	4.82418	0.48427	1.77365
C	2.55944	-0.87477	2.58786
C	3.70537	0.35558	0.94108

H	1.62671	-1.38163	2.84928
N	2.59119	-0.30722	1.35594
H	4.16051	1.84900	-0.57666
C	3.66938	0.86362	-0.47558
H	4.21784	0.15652	-1.12303
H	0.67146	2.34910	-1.16995
N	2.24295	0.96791	-0.97190
Co	1.05705	-0.21619	0.16386
C	1.74840	2.39881	-0.94970
H	1.88186	2.75263	0.08628
H	2.86201	0.73939	-3.03923
N	1.73299	-1.58031	-0.95544
C	2.10675	0.35157	-2.33511
H	1.35735	-3.16276	0.34838
C	1.73950	-2.89875	-0.63959
C	2.20270	-1.14225	-2.16031
C	2.45179	3.33903	-1.91548
C	2.22091	-3.84563	-1.54706
C	2.70165	-2.04839	-3.10009
C	2.70445	-3.41747	-2.79252
N	3.68644	3.76421	-1.54934
H	2.21650	-4.90201	-1.26741
H	3.08544	-1.67717	-4.05430
H	3.09222	-4.14097	-3.51522
H	1.10638	0.61960	-2.71827
H	0.82458	3.39466	-3.36095
C	1.82796	3.75196	-3.10714
C	4.33127	4.60886	-2.37886
H	5.32894	4.93055	-2.05507
C	2.50834	4.64029	-3.95477
C	3.78682	5.07900	-3.58529
H	2.04414	4.98341	-4.88503
H	4.35406	5.77337	-4.21243
O	-0.44286	0.38793	-0.53268
O	-0.02459	-1.08555	1.25357

Table S17. Cartesian coordinates for optimized N-arm in **3** complex.

Co	-1.30528	-0.30036	0.40540
N	-2.68242	-1.18336	1.53505
C	-2.39402	-0.73396	2.93901
H	-1.53748	-1.32537	3.30505
H	-3.25066	-0.92601	3.60663
N	-1.35094	1.09670	1.75800
C	-1.99822	0.72177	2.90017
C	-2.19073	1.62127	3.95241
H	-2.72333	1.29805	4.85098
C	-1.68602	2.92530	3.83211
H	-1.82571	3.64582	4.64343
C	-1.00516	3.28819	2.66254
H	-0.59221	4.29178	2.53111
C	-0.85699	2.34955	1.63339
H	-0.32434	2.58843	0.70059
C	-4.07517	-0.78203	1.09004
H	-4.62556	-0.36466	1.94993
H	-4.62540	-1.68438	0.77304
N	-2.79431	0.54749	-0.49432
C	-4.03028	0.21846	-0.04076
C	-5.18209	0.77666	-0.61038
H	-6.16796	0.49834	-0.22750
C	-5.04494	1.68451	-1.66840
H	-5.93224	2.13087	-2.12688
C	-3.76063	2.01196	-2.13152
H	-3.61145	2.71467	-2.95500
C	-2.65327	1.42277	-1.51930
H	-1.62427	1.63026	-1.82520
C	-2.43889	-2.65495	1.33336
H	-3.28120	-3.25888	1.70999
H	-1.53589	-2.92016	1.90938
N	-1.52968	-1.83842	-0.73966
C	-2.17234	-2.87949	-0.13437
C	-2.50360	-4.03565	-0.84643
H	-3.02513	-4.85265	-0.34062
C	-2.16069	-4.11834	-2.20510
H	-2.41236	-5.01335	-2.78141
C	-1.50848	-3.03776	-2.81621
H	-1.23656	-3.05899	-3.87439
C	-1.21294	-1.90415	-2.05213
H	-0.71927	-1.02144	-2.46686
H	5.48975	-0.08115	4.42643
C	4.71574	-0.16757	3.65817
H	3.18972	-0.96868	4.99777
H	5.96811	0.60459	2.04844
C	3.44147	-0.65907	3.98024
C	4.98699	0.21786	2.33725
C	2.47183	-0.73683	2.97783
C	3.97771	0.09594	1.37683

H	1.45396	-1.09030	3.16091
N	2.73989	-0.36770	1.70062
H	4.93650	1.13920	-0.26865
C	4.17077	0.36679	-0.09011
H	4.53451	-0.55922	-0.56988
H	2.68355	2.62252	0.23908
N	2.85840	0.75752	-0.74461
Co	1.39438	-0.23158	0.30181
C	2.80777	2.28064	-0.80058
H	3.80063	2.61514	-1.15388
H	3.64271	0.35898	-2.72785
N	2.00725	-1.70052	-0.72077
C	2.76515	0.12156	-2.10106
H	1.32214	-3.18310	0.57344
C	1.81260	-3.00032	-0.38411
C	2.62179	-1.36419	-1.89218
C	1.75789	2.94199	-1.67599
C	2.23003	-4.02745	-1.23405
C	3.06323	-2.35413	-2.77477
C	2.85747	-3.70245	-2.44587
N	0.65390	3.41847	-1.05416
H	2.06351	-5.06570	-0.93660
H	3.56699	-2.06344	-3.70051
H	3.19673	-4.49060	-3.12399
H	1.86480	0.52480	-2.59555
H	2.93103	2.80953	-3.50887
C	2.00453	3.16495	-3.04589
C	-0.23603	4.11353	-1.79212
H	-1.11088	4.49450	-1.25051
C	1.06238	3.87423	-3.80466
C	-0.08496	4.36277	-3.16565
H	1.23412	4.05673	-4.87016
H	-0.84079	4.93725	-3.70947
O	0.03957	0.42768	-0.59760
O	0.13671	-1.02222	1.25570

Table S18. Cartesian coordinates for optimized single μ-O **3** complex.

Co	-1.56363	-0.14318	-0.42174
N	-3.45984	-0.22012	-1.17963
C	-3.79457	-1.68382	-1.20182
H	-3.33795	-2.10814	-2.11142
H	-4.88491	-1.84179	-1.25801
N	-2.02368	-1.81377	0.45349
C	-3.18682	-2.36365	0.00040
C	-3.72122	-3.51147	0.59609
H	-4.65846	-3.92937	0.21825
C	-3.04293	-4.10349	1.67113
H	-3.44658	-5.00105	2.14877
C	-1.85196	-3.52359	2.13048
H	-1.29562	-3.94736	2.97031
C	-1.37473	-2.36950	1.50157
H	-0.46137	-1.85962	1.81815
C	-4.42246	0.59425	-0.35531
H	-5.40355	0.09189	-0.31496
H	-4.58017	1.55978	-0.86768
N	-2.53666	0.70881	1.15960
C	-3.87749	0.85901	1.02404
C	-4.68638	1.27825	2.08902
H	-5.76472	1.38700	1.94221
C	-4.09181	1.54671	3.32854
H	-4.70309	1.87486	4.17447
C	-2.70716	1.36914	3.47000
H	-2.20173	1.54719	4.42264
C	-1.96754	0.93785	2.36642
H	-0.89339	0.74462	2.41560
C	-3.33648	0.37181	-2.55095
H	-4.32707	0.58852	-2.98634
H	-2.81932	-0.36730	-3.18543
N	-1.50885	1.52906	-1.46965
C	-2.47299	1.60263	-2.43431
C	-2.59611	2.72715	-3.25702
H	-3.39092	2.76205	-4.00741
C	-1.69477	3.79093	-3.10221
H	-1.77451	4.67858	-3.73646
C	-0.69632	3.69742	-2.12387
H	0.03344	4.49615	-1.96968
C	-0.63823	2.54989	-1.32660
H	0.12952	2.41203	-0.56577
H	2.47791	-5.80647	-0.79320
C	2.32796	-4.72954	-0.67249
H	0.25308	-4.71942	-1.34812
H	4.37155	-4.32182	-0.03321
C	1.09589	-4.13414	-0.97101
C	3.37947	-3.91068	-0.24066
C	0.93409	-2.75868	-0.77950
C	3.16387	-2.53677	-0.09459

H	-0.00383	-2.24303	-1.04983
N	1.93706	-1.97105	-0.32014
H	4.99691	-1.97699	0.93506
C	4.28693	-1.57902	0.19038
H	4.85672	-1.42002	-0.74186
H	3.54388	-0.99969	2.61296
N	3.73826	-0.25822	0.64571
Co	1.76681	-0.13539	0.27800
C	3.89806	-0.07552	2.12135
H	4.96018	0.06719	2.38997
H	5.46466	0.72436	-0.21124
N	2.38657	0.54040	-1.40235
C	4.37684	0.88043	-0.11307
H	0.62391	0.07816	-2.43860
C	1.63569	0.51238	-2.52934
C	3.67835	0.97626	-1.44176
C	3.04363	1.09665	2.52204
C	2.15012	0.98113	-3.74329
C	4.24695	1.44685	-2.62818
C	3.46547	1.46404	-3.79371
N	1.96748	1.30186	1.70647
H	1.51964	0.95103	-4.63581
H	5.28721	1.78347	-2.63420
H	3.88967	1.82852	-4.73392
H	4.22326	1.80826	0.46397
H	4.18249	1.70511	4.25356
C	3.30630	1.90653	3.63109
C	1.13726	2.33274	1.98870
H	0.27992	2.45171	1.32662
C	2.43764	2.96937	3.91757
C	1.33713	3.18710	3.07715
H	2.62405	3.61997	4.77697
H	0.63598	4.00700	3.25199
O	0.03169	0.10021	0.43515
O	-1.01164	-0.97664	-1.82886

Table S19. Cartesian coordinates for optimized *cis*-**2** – triplet state.

Co	-2.00420	-0.57955	0.48182
N	-3.51402	-1.26001	1.58507
C	-3.24741	-0.71907	2.95922
H	-2.43054	-1.32351	3.38878
H	-4.13039	-0.80485	3.61626
N	-2.02147	0.91408	1.68936
C	-2.76780	0.70622	2.81228
C	-3.01151	1.73548	3.72629
H	-3.62197	1.54215	4.61301
C	-2.46968	3.00703	3.47711
H	-2.65517	3.83033	4.17357
C	-1.69968	3.20755	2.32264
H	-1.26682	4.18433	2.08998
C	-1.49119	2.13307	1.44988
H	-0.89499	2.20814	0.53658
C	-4.83399	-0.77328	1.03073
H	-5.38443	-0.23190	1.81929
H	-5.45537	-1.64379	0.75762
N	-3.35267	0.30910	-0.57260
C	-4.63826	0.12040	-0.17580
C	-5.70555	0.71984	-0.85793
H	-6.73200	0.55212	-0.51815
C	-5.43458	1.52719	-1.97120
H	-6.25408	2.00350	-2.51783
C	-4.10210	1.71548	-2.37277
H	-3.84919	2.33791	-3.23528
C	-3.08521	1.08996	-1.64817
H	-2.02374	1.18660	-1.89671
C	-3.38856	-2.75316	1.50475
H	-4.29846	-3.26372	1.86589
H	-2.54323	-3.03975	2.15274
N	-2.28432	-2.17443	-0.55393
C	-3.05143	-3.11148	0.07548
C	-3.44415	-4.28605	-0.57349
H	-4.06697	-5.01514	-0.04746
C	-3.03355	-4.50062	-1.89922
H	-3.33118	-5.41155	-2.42719
C	-2.25276	-3.52711	-2.53894
H	-1.92270	-3.65100	-3.57378
C	-1.90068	-2.37014	-1.83469
H	-1.30036	-1.56529	-2.26759
O	-0.51716	-0.00673	-0.46165
O	-0.65751	-1.41924	1.45925
H	2.65354	-6.23135	-1.44002
C	2.32656	-5.22606	-1.15678
H	2.68271	-5.50962	0.97627
C	2.33948	-4.83078	0.18962
H	1.90254	-4.56860	-3.19450
C	1.90892	-4.30799	-2.13247

C	1.91368	-3.53696	0.51669
C	1.50335	-3.03156	-1.72462
H	2.63163	-3.48615	2.56973
C	1.87634	-2.99538	1.92706
N	1.49499	-2.65330	-0.42614
H	0.87803	-3.16711	2.36831
H	1.18435	-2.27528	-2.44868
H	3.85653	-2.01558	0.86670
N	2.06809	-1.50884	1.89789
C	3.45009	-1.15292	1.42362
Co	0.71039	-0.87837	0.47702
C	3.39858	0.03667	0.49338
C	4.50874	0.84191	0.21394
H	5.45559	0.65923	0.73091
N	2.19738	0.23715	-0.12033
H	0.67932	-1.06265	3.39317
C	1.77475	-0.98802	3.28585
C	4.38578	1.87291	-0.72957
H	4.13085	-0.97571	2.27416
C	2.07716	1.24024	-1.02508
H	2.25468	-1.66379	4.01903
C	3.14854	2.07127	-1.36202
H	5.24208	2.51338	-0.96232
H	1.07628	1.35257	-1.45322
H	3.00724	2.86479	-2.10109
C	2.23719	0.43049	3.55884
N	1.56822	1.43094	2.93730
C	1.94816	2.69665	3.20177
C	3.29029	0.67204	4.46295
H	1.38389	3.48287	2.68470
H	3.79863	-0.16476	4.95378
C	2.98581	3.03442	4.08631
C	3.66973	1.99600	4.73182
H	3.24220	4.08372	4.26246
H	4.48318	2.20873	5.43325

Table S20. Cartesian coordinates for optimized *trans*-**2** – triplet state.

Co	-1.87193	-0.53371	0.79368
N	-3.37757	-1.30104	1.86530
C	-3.14151	-0.77193	3.24898
H	-2.28253	-1.32954	3.65922
H	-4.01422	-0.92403	3.90875
N	-2.02640	0.95017	1.99790
C	-2.75822	0.68469	3.11871
C	-3.08558	1.69360	4.02949
H	-3.67952	1.45397	4.91622
C	-2.65026	3.00526	3.77634
H	-2.90015	3.81168	4.47255
C	-1.90847	3.26775	2.61548
H	-1.56070	4.27698	2.37869
C	-1.61647	2.21222	1.74362
H	-1.03776	2.32512	0.82257
C	-4.70495	-0.84766	1.30457
H	-5.25053	-0.28157	2.07962
H	-5.32554	-1.72964	1.06819
N	-3.24469	0.27331	-0.29430
C	-4.52759	0.01469	0.07021
C	-5.60745	0.53189	-0.65818
H	-6.63237	0.30980	-0.34584
C	-5.35099	1.33051	-1.78167
H	-6.18058	1.74311	-2.36390
C	-4.02036	1.59232	-2.14758
H	-3.78012	2.21077	-3.01676
C	-2.99039	1.04503	-1.37912
H	-1.92646	1.19463	-1.59127
C	-3.19196	-2.78419	1.75589
H	-4.08406	-3.34152	2.09202
H	-2.34353	-3.04884	2.40965
N	-2.06157	-2.12494	-0.26159
C	-2.82049	-3.09614	0.32399
C	-3.18101	-4.25523	-0.36989
H	-3.79634	-5.01417	0.12191
C	-2.75027	-4.41387	-1.69776
H	-3.02593	-5.30992	-2.26224
C	-1.97808	-3.40483	-2.29132
H	-1.63121	-3.48778	-3.32483
C	-1.65274	-2.26858	-1.54111
H	-1.04654	-1.44033	-1.91892
O	-0.41216	0.13249	-0.13209
O	-0.51690	-1.29814	1.81110
H	2.74062	4.20998	4.07045
C	2.35331	3.33656	3.53631
H	3.27061	3.86442	1.62777
C	2.64934	3.15011	2.17699
H	1.32557	2.48594	5.26342
C	1.56858	2.38199	4.20206

C	2.13617	2.01791	1.52869
C	1.09958	1.27737	3.47924
H	3.22918	2.23747	-0.34618
C	2.35417	1.70067	0.06618
N	1.37124	1.10436	2.16954
H	1.45642	2.00259	-0.50247
H	0.48615	0.49795	3.94288
H	4.40894	0.54128	0.79264
N	2.48329	0.22495	-0.10357
C	3.76524	-0.30396	0.49002
Co	0.88080	-0.64749	0.91701
C	3.53141	-1.22349	1.67681
C	4.59865	-1.76569	2.40554
H	5.62753	-1.51786	2.12562
N	2.23671	-1.50771	1.99737
H	1.42515	0.35081	-1.90496
C	2.34071	-0.14834	-1.53995
C	4.33230	-2.61903	3.48610
H	4.32392	-0.85133	-0.29013
C	1.97864	-2.32979	3.04691
H	3.20050	0.20514	-2.13952
C	2.99563	-2.90479	3.81129
H	5.15449	-3.05070	4.06507
H	0.91405	-2.49602	3.24163
H	2.74081	-3.56223	4.64745
C	2.16364	-1.64667	-1.64530
N	1.46425	-2.18682	-0.62023
C	1.25605	-3.51965	-0.60301
C	2.66662	-2.42189	-2.70010
H	0.69815	-3.90691	0.25607
H	3.23509	-1.94964	-3.50752
C	1.72233	-4.36790	-1.61649
C	2.43460	-3.80584	-2.68675
H	1.53215	-5.44360	-1.56155
H	2.81743	-4.43748	-3.49464

Table S21. Cartesian coordinates for optimized *cis*-**3** – quadruplet state.

Co	-1.85308	-0.43952	0.68332
N	-3.33610	-1.28897	1.68988
C	-3.11787	-0.87306	3.11849
H	-2.26555	-1.45852	3.50242
H	-4.00213	-1.09046	3.74113
N	-2.05059	0.96914	2.00069
C	-2.75826	0.59179	3.10574
C	-3.10070	1.51538	4.09723
H	-3.67482	1.18771	4.96808
C	-2.71324	2.85539	3.94150
H	-2.97476	3.59542	4.70335
C	-2.01173	3.23582	2.78894
H	-1.71073	4.27253	2.61913
C	-1.70197	2.26319	1.83272
H	-1.17675	2.49793	0.90438
C	-4.67112	-0.81020	1.15597
H	-5.23725	-0.33557	1.97499
H	-5.26444	-1.68066	0.82799
N	-3.22501	0.45888	-0.34537
C	-4.50178	0.16619	0.01178
C	-5.58866	0.74989	-0.65236
H	-6.60934	0.50043	-0.34836
C	-5.34326	1.64704	-1.70019
H	-6.17891	2.11270	-2.23078
C	-4.01793	1.93993	-2.05982
H	-3.78588	2.63374	-2.87166
C	-2.97919	1.32485	-1.35861
H	-1.92360	1.50334	-1.58451
C	-3.14032	-2.76575	1.48117
H	-4.02799	-3.33931	1.79650
H	-2.28434	-3.07285	2.10544
N	-2.07680	-1.94477	-0.51000
C	-2.80154	-2.96939	0.02643
C	-3.17695	-4.07276	-0.74508
H	-3.76149	-4.87758	-0.29140
C	-2.80760	-4.11272	-2.09864
H	-3.09660	-4.96355	-2.72237
C	-2.08689	-3.04106	-2.64437
H	-1.79731	-3.02484	-3.69800
C	-1.74008	-1.96707	-1.81808
H	-1.19267	-1.09423	-2.18249
O	-0.35119	0.22781	-0.14800
O	-0.54283	-1.26906	1.65595
H	2.53237	-5.97897	-1.64133
C	2.20801	-5.00586	-1.26019
H	2.60121	-5.48477	0.83110
C	2.24213	-4.73854	0.11618
H	1.76818	-4.15554	-3.22176
C	1.78276	-3.99978	-2.13981

C	1.82032	-3.48094	0.56846
C	1.38123	-2.76798	-1.60814
H	2.55367	-3.65957	2.61101
C	1.83911	-3.06077	2.01868
N	1.37758	-2.52165	-0.28095
H	0.83388	-3.18231	2.45885
H	1.07031	-1.94486	-2.25713
H	4.09051	-2.28379	1.40384
N	2.17370	-1.60375	2.08992
C	3.59271	-1.32714	1.63907
Co	0.87460	-0.62589	0.82763
C	3.66305	-0.41113	0.43251
C	4.88806	-0.01893	-0.12438
H	5.82421	-0.37673	0.31430
N	2.48740	0.02077	-0.09649
H	0.90469	-1.42548	3.75927
C	1.91256	-1.07973	3.46903
C	4.89117	0.82980	-1.23942
H	4.15829	-0.88203	2.47598
C	2.48385	0.84306	-1.17240
H	2.64137	-1.48788	4.19192
C	3.66973	1.27009	-1.77351
H	5.83899	1.14506	-1.68593
H	1.49472	1.14404	-1.53099
H	3.63100	1.93323	-2.64141
C	1.94675	0.42914	3.42632
N	1.46228	0.95667	2.27636
C	1.50662	2.29262	2.09158
C	2.45018	1.23396	4.45696
H	1.15827	2.65883	1.12154
H	2.83864	0.77448	5.37048
C	1.99487	3.16483	3.07203
C	2.46050	2.62554	4.28046
H	2.01400	4.24126	2.88224
H	2.85027	3.27777	5.06781

Table S22. Cartesian coordinates for optimized *trans*-**3** – quadruplet state.

Co	-1.56960	-0.48540	0.72787
N	-3.16139	-1.30342	1.76631
C	-3.02750	-0.85091	3.18687
H	-2.13848	-1.35536	3.60565
H	-3.90677	-1.15042	3.78441
N	-2.07256	1.10517	2.16258
C	-2.81976	0.64736	3.19660
C	-3.33621	1.50979	4.17242
H	-3.94287	1.11182	4.99111
C	-3.06772	2.88316	4.06619
H	-3.46190	3.57972	4.81232
C	-2.30572	3.35226	2.98559
H	-2.08660	4.41607	2.86150
C	-1.82630	2.42726	2.04999
H	-1.23215	2.73519	1.18399
C	-4.45710	-0.81669	1.15214
H	-5.04957	-0.29643	1.92465
H	-5.05736	-1.68753	0.83635
N	-2.95450	0.38228	-0.37227
C	-4.23954	0.10786	-0.02684
C	-5.31085	0.66613	-0.73806
H	-6.33848	0.43369	-0.44403
C	-5.04340	1.51606	-1.81921
H	-5.86787	1.95937	-2.38561
C	-3.71064	1.79112	-2.16521
H	-3.46130	2.44896	-3.00163
C	-2.68945	1.20416	-1.41587
H	-1.62773	1.36943	-1.62322
C	-3.03091	-2.78987	1.65964
H	-3.91379	-3.29826	2.08663
H	-2.14645	-3.08129	2.25326
N	-2.07111	-2.25344	-0.48128
C	-2.81516	-3.15341	0.20714
C	-3.32123	-4.31062	-0.39919
H	-3.92485	-5.01457	0.18081
C	-3.04550	-4.53435	-1.75675
H	-3.43122	-5.42836	-2.25601
C	-2.28745	-3.59176	-2.46752
H	-2.06328	-3.72382	-3.52930
C	-1.81902	-2.45876	-1.79134
H	-1.22738	-1.68898	-2.29637
O	-0.18481	0.20778	-0.13106
O	-0.30708	-1.25876	1.70946
H	2.28356	4.10901	4.08759
C	2.01747	3.22776	3.49670
H	3.02559	3.91007	1.68545
C	2.43129	3.12423	2.15946
H	0.94624	2.22056	5.10925
C	1.27625	2.18364	4.06820

C	2.08239	1.98424	1.42972
C	0.96116	1.06810	3.28545
H	3.33102	2.29552	-0.33656
C	2.44155	1.72968	-0.01284
N	1.34757	0.98137	1.99311
H	1.59166	2.01598	-0.65545
H	0.39047	0.21993	3.67091
H	4.58143	0.67192	0.64833
N	2.64065	0.24843	-0.17279
C	3.97819	-0.20995	0.37328
Co	1.15822	-0.57324	0.85731
C	3.81137	-1.12626	1.56542
C	4.89816	-1.66533	2.26635
H	5.91902	-1.42066	1.95933
N	2.53464	-1.41528	1.92473
H	1.56637	0.34347	-1.98840
C	2.42479	-0.22030	-1.58527
C	4.65226	-2.51354	3.35403
H	4.53109	-0.73232	-0.42562
C	2.28820	-2.23443	2.97596
H	3.30607	-0.01837	-2.21734
C	3.32672	-2.80360	3.71509
H	5.48767	-2.94362	3.91424
H	1.23222	-2.41292	3.19939
H	3.09431	-3.46007	4.55732
C	2.07389	-1.68630	-1.51962
N	1.35581	-2.02308	-0.40816
C	0.98264	-3.30589	-0.20461
C	2.41762	-2.64504	-2.47669
H	0.42462	-3.50038	0.71437
H	2.99916	-2.35029	-3.35439
C	1.29413	-4.31135	-1.12588
C	2.01710	-3.97599	-2.27944
H	0.97419	-5.33773	-0.93012
H	2.27978	-4.74314	-3.01360